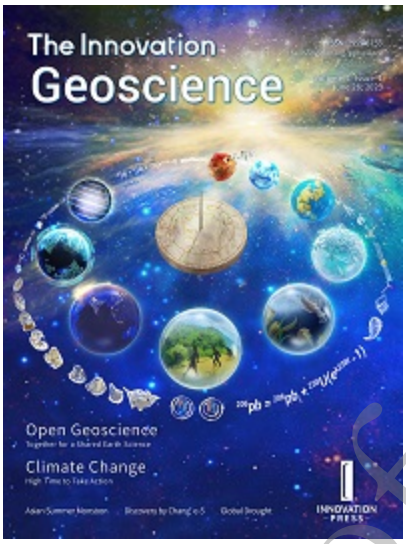

AMS ^{14}C dating with biochemical characterization by pyrolysis-combustion and infrared technology reveal terrestrial organic carbon cycling dynamics

Journal:	*The Innovation Geoscience*
Manuscript ID	XINNgeoscience-2025-0204.R3
Manuscript Type:	Article
Keywords:	Advanced radiocarbon dating, Terrestrial organic carbon cycling dynamics, Pyrolysis-combustion technology, Partition of thermally labile and stable organic compounds, Characterization of labile, recalcitrant and stable fractions, Function groups of thermally labile and stable fractions, Subtropical and temperate climate zones

AMS ^{14}C dating with characterization by pyrolysis and infrared technology reveal terrestrial organic carbon cycling dynamics

Hong Wang[1,2]*, Xiaofei Gao[1], Yi Yang[1], Peng Cheng[2,6]*, Jia Cao[1], Dongxue Li[3], Peixian Shu[2], Guodong Ming[4], Yingna Liu[1], Keli Zhang[1], Baoshan Cui[3], Yongming Han[2], Xuefeng Lu[2], Hua Du[2], Feng Xian[2], Xiaolin Hou[2], Sanyuan Zhu[5], Yanmin Sun[5], Tianhe Liu[1], Lin liu[1], Xiaolei Zhao[1], Weijian Zhou[2], Zhisheng An[2]

[1] State Key Laboratory of Earth Surface Process and Disaster Rick Reduction, Faculty of Geographical Science, Beijing Normal University, Beijing 100875, China
[2] State Key Laboratory of Loess and Quaternary Geology, Xi'an 710061, China.
[3] School of Environment, State Key Joint Laboratory of Environmental Simulation and Pollution Control, Beijing Normal University, Beijing 100875, China
[4] Institute of Deep Space Sciences, Deep Space Exploration Laboratory, Hefei 230088, China
[5] State Key Laboratory of Organic Geochemistry, Guangzhou Institute of Geochemistry, Chinese Academy of Sciences, Guangzhou 510640, China.
[6] Institute of Global Environmental Change, Xi'an Jiaotong University, Xi'an 710049, China
*Correspondence: hongwang@bnu.edu.cn (H.W.);chp@ieecas.cn (P.C.)

Graphical Abstract

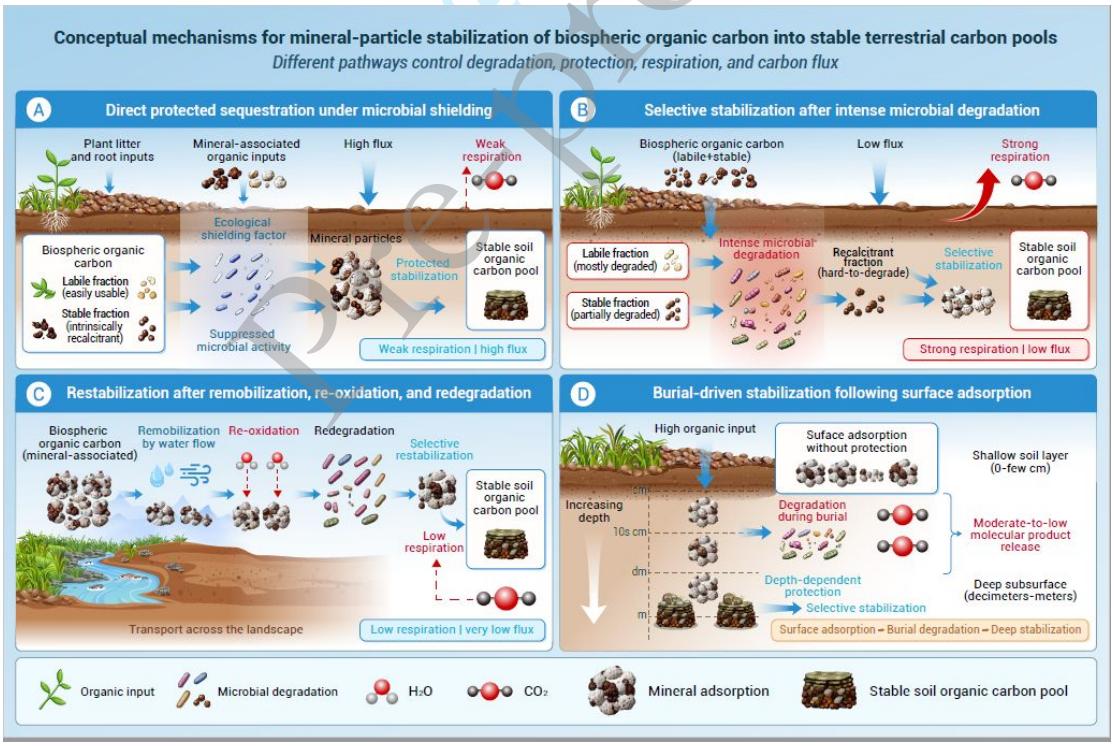

Public summary

- The updated pyrolysis system successfully partitions thermally labile and stable organic carbon fractions.
- Their AMS ^{14}C age patterns demonstrate terrestrial carbon cycling dynamics that are known only in models.
- Their reverse older-younger/identical age patterns exhibit protective preservation under weak respiration.

- Their constant younger-older age patterns exhibit selective preservation under intensive organic degradation.
- Their identical modern to younger-older age patterns across depth reveal organic carbon fixation dynamics.

Key Words：

- Updated pyrolysis technology
- Partition of organic carbon components
- Terrestrial carbon dynamics

ABSTRACT

Terrestrial systems hold twice as much organic carbon (OC) as the atmosphere and vegetation combined. The long-term stability of this carbon pool influences ecological resilience and helps mitigate global climate change. Here, we couple an updated pyrolysis-combustion system with online infrared gas analyzer (IRGA) and Fourier transform infrared spectroscopy (FTIR) to partition OC into thermally labile, recalcitrant, and stable fractions, enabling the analysis of their biochemical structures, origins, and AMS ^{14}C ages. We find that the labile-recalcitrant and stable OC fractions from fluvial, eolian, and farmland ecosystems consistently exhibit younger-to-older age patterns over timescales ranging from 10^2 to 10^4 year. These trends exhibit a first order reaction rate temperature dependance as predicted by Arrhenius equation. This pattern verifies selective preservation of OC compounds by minerals under microbial respiration. In contrast, labile-recalcitrant and stable OC fractions from rock varnish and flooding sediments in karst cracks and sinkholes exhibit reverse (older-younger) or identical age patterns, confirming protection of OC by minerals in the absence of intensive respiration. In high-organic-carbon-stock ecosystems, thermally labile-recalcitrant and stable OC fractions yield identical modern ages in the rhizosphere and younger-to-older age patterns in deeper zones, quantitatively exemplifying the process by which unprotected OC progressively attaches to mineral-associated forms. The CO_2 thermograms from IRGA and the OC functional

groups from FTIR analysis provide biochemical evidence for assessing the origin of terrestrial OC compounds, thereby improving our understanding of their age patterns. We conclude that pyrolysis-combustion technology holds significant potential for revealing the mechanisms underlying terrestrial OC preservation.

INTRODUCTION

Terrestrial systems hold twice as much organic carbon (OC) as found in the atmosphere and vegetation combined,[1] influencing food productivity, soil erosion, and climate change mitigation. Microbes and enzymes decompose and respire labile OC compounds (e.g., starch and sugars), into atmosphere,[2-4] whereas structurally and energetically recalcitrant OC compounds (e.g., lignin and humin) can survive this process[5]. However, experimental results suggest that chemical structures alone do not regulate soil OC stability, turnover times, or preservation dynamics; rather, ecosystem factors also constrain decomposition rates and protective pathways. For example, soil microaggregates and pore spaces can shield organic carbon from decomposition, [5] and the low activity of microbes and enzymes in semi-arid bioclimate zones can slow decomposition rates, whereas high fluxes of dissolved organic carbon can increase OC content in organo-mineral associations within lower soil horizons. [6] To enhance the storage of carbon in terrestrial ecosystems and to sequester atmospheric CO_2 for climate change mitigation, stabilizing biosphere OC is crucial. To date, however, no models have succeeded in predicting soil OC stability and turnover times across different bioclimate zones. [7–8]

A key challenge in quantifying the stability and turnover times of different OC components, such as labile and recalcitrant compound groups, for accelerator mass spectrometry (AMS) ^{14}C dating is how to effectively partition these fractions. Wet

chemistry[9–11] and ramped thermal decomposition under low oxygen flow rates[12–17] are commonly used for this purpose. This approach assumes that more intensive procedures, stronger chemical doses, and higher temperature pretreatments yield progressively more recalcitrant organic carbon fractions.[18–20] However, these techniques only marginally or are even incapable of achieving this goal.[5,21–28] Although humification and mineral protection can produce biochemically stable geopolymers that resist chemical and thermal treatment,[7–8,29] the recycling of stabilized organic carbon can also fragment and simplify these geopolymers, making them susceptible to such treatments.[11,30–31] Consequently, the "recalcitrant" organic carbon components defined by wet chemistry or low-oxygen combustion become ambiguous, complicating discussions of terrestrial OC stability and cycling dynamics.[6, 32–33] Here, we interfaced an updated pyrolysis-combustion devise, originally for conventional ^{14}C dating, [34-37] with an online IRGA and gas-phase FTIR for AMS ^{14}C dating of thermally-sensitive terrestrial OC fractions with biochemical structure information to evaluate the origin and evolution of terrestrial OC compound stability (Figure S1). This pyrolysis-combustion device updates currently the popular apparatus of ramped pyrolysis and low O_2 content oxidation, known as RPO, technology[26-27] in that pyrolysis products (volatile compounds) are purged from the pyrolysis (inner) tube into combustion (outer) tube by Ar gas via an orifice for instant O_2 combustion in outer tube (Figure S1). This design prevents volatile compounds from traveling long distances and interacting with one another. In addition, the higher Ar gas pressure caused by restricted gas flow at the tip of the inner tube further inhibits O_2 backflushing. By partitioning thermally labile-recalcitrant (O_2-free) and stable (with O_2) compounds, this approach generates multiple thermally sensitive CO_2 aliquots for AMS ^{14}C dating analysis (Figure S1). Finally, CO_2 thermograms recorded by the online IRGA and OC functional groups

identified by FTIR spectra provide biochemical structure information for evaluating the origin and evolution of these thermal fractions.

Using this novel technology, we investigated a range of terrestrial systems: current Yellow River deltaic fluvial deposits, western Chinese loessland eolian silt in semi-arid regions, high-closure volcanic lacustrine sediments, black (mollisol) farmland in semi-humid Northeast China, and karst rock varnish veneers in subtropical Southwest China (Figure S2). We further compiled ^{14}C dates from thermally labile-recalcitrant and stable organic carbon fractions derived from flood deposits in caves fed by karst cracks and sinkholes, as well as from a critical zone observatory engineered soil profile in humid central United States and silvergrass farmland soil in subtropical Japan (Figure S2). Together, these data provide benchmarks for verifying terrestrial organic carbon preservation dynamics that have previously been observed only in modeling simulations.

MATERIALS AND METHODS

Sample sites and materials

Terrestrial sediment and soil profiles are collected in Northern Hemisphere middle latitudes for AMS ^{14}C dating on thermally sensitive OC fractions. They include the current Yellow River deltaic floodplain in east coast of China, loess from western Chinese Loess Platea, rock varnishes on newly exposed limestone bedrocks in erosive karst region in SW China, organic-rich mollisol farmland and high-closure lacustrine in NE China. The ^{14}C dates of thermally sensitive OC fractions of flooding sediment sequence in caves in karst region from the central USA, high OC stock grassland farms from S. Japan and engineered soil at the Critical Zone Observatory site from the central USA are compiled for discussion.

Yellow River deltaic sediment: A 21 m long core was collected by percussion corer from current delta near the Bohai Sea coast area at 38°02'N, 118°53' E (Figure 1A). Subsamples were taken in 0.9-1.0 m, 4.8-4.9 m, 10.2-10.3m, 15.6-15.7 m, 20.9-21m intervals.

Loess profile: A 13m loess section was sampled from western Chinese Loess Plateau in Gansu Province at 36°20'47" N, 107°20'54" E. Subsamples were taken in 0.5 m increments from 3 to 12.5 m depths (Figure 1B).

Rock varnishes: Rock varnish sequence was scraped in 20 cm increments from 1.2m high limestone rock above sparse bushland surface from the karst Mountain region in the SW China at 25.5 °N, 105.75 °E (Figure 1C1-C2).

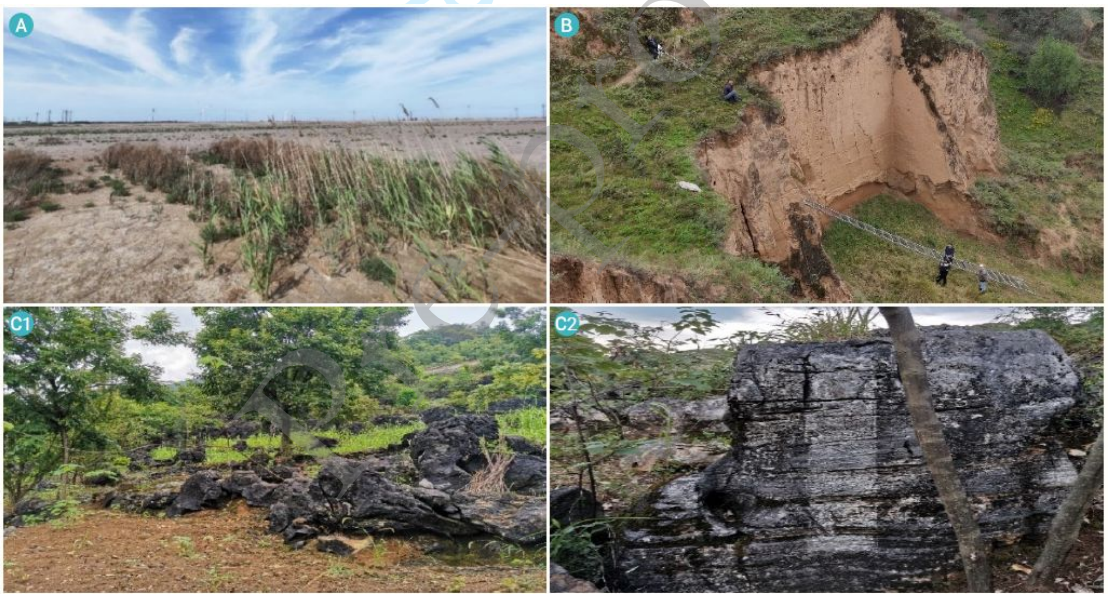

Figure 1. Field views of Yellow River deltaic floodplain, semi-arid western Chinese Loess Plateau, and warm-humid subtropic karst ecosystems A. Current Yellow River delta. **B**. A loess profile from western Chinese Loess Plateau. **C1-2**. Karst geomorphology and rock varnish veneers on bedrock surfaces.

Mollisol farmland soil profiles: A total of 16 mollisol samples from 4 farmland sections in the Jiutai (JT) City areas in NE China by a hand auger. Soil samples were taken in 20 cm increments from the JT#23, #26, and #32 sites, and 0-20, 37-57, 90-100, 144-164 cm depth intervals from the #28 site. They are located at 44°00′00″N, 125°48′

00″E for JT #23; at 44°12′00″N, 125°36′00″E for JT#26; at 44°12′00″N, 126°00′00″E for JT#28; and at 44°24′00″N, 126°12′00″E for JT#32 soil profile (Figure. 2A).

High-closure Mountain Forest volcanic lake sediment: Several frozen cores were collected from the freezing Lake Sihailongwan (SHLW) in NE China (42°17′24″N, 126°35′51″E, Figure 2B) using a freeze corer (UWITEC GmbH, Austria) in 2022. These cores were immediately stored in a mobile freezer (−36°C) and transported to the Institute of Earth Environment, Chinese Academy of Sciences (IEECAS) in Xi'an for Anthropocene and to Faculty of the Geography at the Beijing Normal University for OC cycling dynamic studies. They have been stored in a freezer under –20°C and subsamples were taken in 1 cm increment from 0 to 8.5 cm depths that spins from AD 1950 to AD 2020.

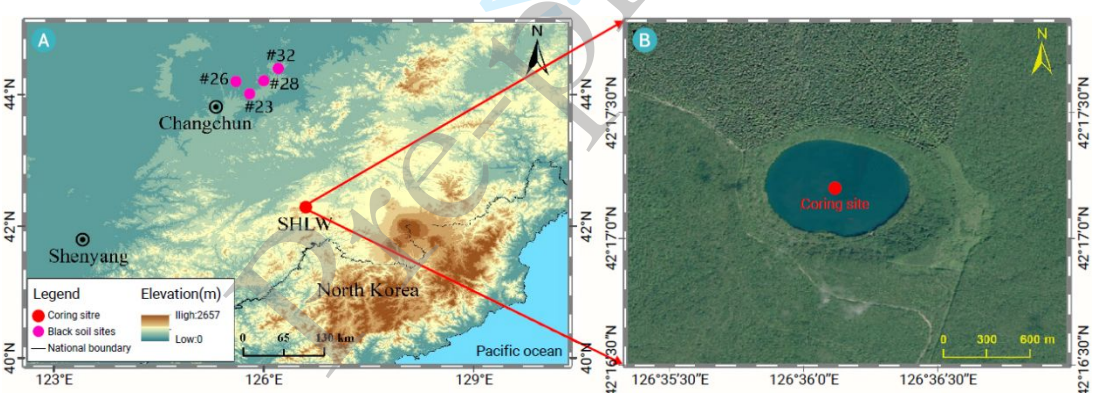

Figure 2. Location of four mollisol farmland sites and the high-closure mountain forest volcanic lake (Lake Sihailongwan, SHLW). **A**. Mollisol farmland selected for carbon cycling studies in Jilin Province, NE China. **B**. High-closure Mountain Forest volcanic lake sediment selected for air-born OC cycling studies.

Experimental analysis

Chemical pretreatment: About 2-5g of soil and sediment or 0.5g of rock varnish samples from different terrestrial ecosystems were pretreated by using hot 2 M HCl at 80°C for 2 hours, rinsed to neutrality using ultra-pure Mili-Q water, oven-dried at 70°C overnight.

Thermally sensitive OC fractional characterization: For sediment/soil specimens, about 0.2-0.5g and for rock varnish specimen 0.01-0.02g rock varnish samples were weighted and transferred into the inner pyrolysis quartz tube or a small quartz glass boat in the inner tube (Figure S1A). When combustion furnace reaches to 750°C, Ar gas is purged into inner tube and O_2 gas is purged into outer quartz tube, and flow-control valve is adjusted to maintain total pressure at 1.5 psi with Ar pressure is slightly greater than O_2 pressure and Ar gas flows at 80ml/min and O_2 flows at 50ml/min. Then, pyrolysis furnace increases temperature from 40°C to 750°C in 35 minutes and ramped rate is ~20°C/min. The CO_2 thermogram of thermally labile-recalcitrant OC fraction is captured by the online IRGA monitored. After pyrolysis process is completed, the pyrolysis furnace is shut off and wait until it reaches room temperature. This procedure is repeated for thermally stable OC fraction through replacing Ar gas by O_2 in the inner tube. The CO_2 thermogram of thermally stable OC fraction is captured by the online IRGA.

Thermally sensitive OC compounds functional group analysis: Repeat the above procedure with combustion furnace set at 120°C and no O_2 gas in the outer tube. As pyrolysis furnace ramps up from 40°C to 750°C, the absorbance bands and intensity are recorded by the online FTIR spectroscopy (Figure S1A).

Partition of thermally labile-recalcitrant OC fractions by pyrolysis: 1-3g pretreated and oven dried sediment/soil samples are accurately weighed into the inner tube or 0.05-0.15g of rock varnish samples are weighed in a small quartz boat and insert the boat into the inner tube. After the pyrolysis-combustion system is evacuated to 1-2 mTorr level, the combustion furnace is switched on. When it reaches to 750°C, the flow-control valve next to the compound gage is shut off and Ar gas is purged into inner tube and O_2 gas is purged into outer tube (Figure S1A). Then, flow-control valve is

adjusted to maintain pressure at 1.5 psi with Ar gas flow rate at 80ml/min and O_2 flow rate at 50ml/min with Ar gas pressure is slightly greater than O_2 pressure. After the pyrolysis furnace reaches to 750°C and Ar/O_2 air flows are established, the pyrolysis furnace is moved to wrap the sample. Pyrolysis can be conducted at 450°C and 750°C to isolate thermally labile and thermally recalcitrant organic carbon fractions on two peaks of CO_2 thermogram, which together constitute the composite labile-recalcitrant OC fractions of samples on one peak of CO_2 thermogram. Organic compounds that are thermally decomposed from samples are carried by Ar gas from inner to outer tubes via the orifice (Figure S1A), where O_2 gas at consistent 750°C combusts OC molecules to CO_2. The CO_2 and other combustion gases pass through a cupric oxide and copper/silver furnaces at 750ºC and a double-loop cold trap for purification, cryogenically collection, measurement, and storage in glass tubes separately.

Partition of thermally stable fraction by combustion of pyrolysis residue: After the pyrolysis, the inner quartz tube is filled with O_2 gas by switching valve to disconnect Ar and connect O_2 supplies to combust the pyrolysis residue at 750ºC with O_2 flows of 80 ml/m in the inner and 50 ml/m in the outer tubes. The inert OC fractional CO_2 with other combustion gases pass through the cupric oxide and copper furnaces at 750ºC and multiple traps again and is purified cryogenically, measured, and stored in glass tubes separately.

AMS ^{14}C dating: A dozen of reference samples was also processed through the pyrolysis-combustion vacuum system along with studying samples for QA/QC of the dating analysis, e.g., the NIST Oxalic Acid II, the FIRID wood, IAEA C5 (Two Creek Forest) wood, and deadwood blanks were processed at the same time. Aliquot of CO_2 of thermally sensitive OC fractions is used for graphitization using the in-house hydrogen-iron reduction method for AMS ^{14}C dating analysis. The AMS measurement

was conducted at the AMS center in the Institute of the Earth Environment, Chinese Academy of Science, the Guangzhou Institute of Geochemistry, Chinese Academy of Science, and Beijing Normal University (BNU). Results were corrected online for isotopic fractionation according to the conventions of Stuiver and Polach. Sample preparation backgrounds were subtracted based on the measurements from deadwood blanks with pMC (percent of modern carbon) values ranging from 0.25-0.30. All ^{14}C dates were calibrated using the online IntCal20 (Calib 8.2).

RESULTS

Characterization of thermal fractions

The CO_2 thermogram of thermally labile-recalcitrant fractions, defined by pyrolysis, and stable fractions, defined by combustion, can be characterized using Rock-Eval technology.[38-41] The CO_2 fluxes released from OC materials during ramped pyrolysis and combustion in 20 °C/min are comparable to CO_2 thermograms from hydrocarbon decomposition, biopolymer cracking, geopolymer cracking, and charred products obtained by Rock-Eval analysis (Table S1).[42-45] Here, we propose that thermally labile-recalcitrant OC compounds likely derive from ancient volatile-containing organic carbon (e.g., animal protein residues and petroleum vapors), while thermally stable OC compounds correspond to elemental carbon. For example, the thermally stable fraction is dominant in anthracite, whereas the thermally labile-recalcitrant fraction is overwhelmingly dominant in glycerin, reflecting naturally formed high- and low-molecular-weight OC compounds, respectively (Figures 3A-B). Conversely, the CO_2 thermograms of thermally stable fractions from lignin and fulvic materials may reflect charred materials originating from labile-recalcitrant fractions (Figures 3C-D). The identification of thermally stable OC compounds as charred

materials, naturally formed elemental carbon, or high molecular weight OC compounds, can be determined through AMS ^{14}C dating analysis. Specifically, overlapping AMS ^{14}C ages between the thermally labile-recalcitrant and stable OC fractions reflect a common origin, otherwise they reflect different origins.

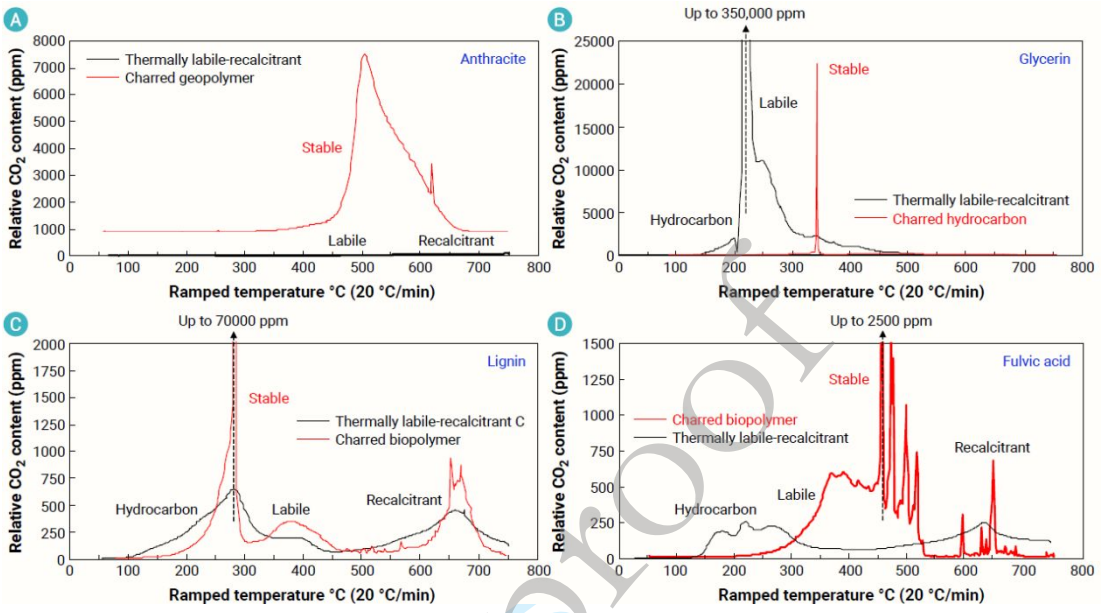

Figure 3. The CO_2 thermogram of selected OC reference materials on ramped temperatures of pyrolysis-combustion method. Pyrolysis generates thermally labile from hydrocarbon decomposition and biopolymer cracking and thermally recalcitrant from geopolymer cracking fractions. Combustion of pyrolysis residue generates thermally stable fractions. **A.** anthracite; **B.** glycerin; **C**. lignin; **D**. fulvic acid.

^{14}C age patterns to show selective preservation dynamics

The Yellow River course has undergone six large-scale changes, with the most recent occurring since AD 1850. [46–47] AMS ^{14}C dating of current Yellow River deltaic sediments at depths of 0–20 m (Figure 1A) provides quantitative data to assess whether ancient or modern carbon is being sequestered in the coastal region in response to global changes (Figure 4A).

Notably, the thermally labile-recalcitrant and stable OC fractions are 4,000–14,000 years older than the AD 1850 reference, while the labile-recalcitrant OC fractions are approximately 10,000 years younger than the thermally stable fractions (Table S2). Similarly, in the last glacial loess-paleosol sequence in western Chinese

Loess Plateau (Figure 1B) thermally labile-recalcitrant fractions are approximately 20,000 years younger than thermally stable OC fractions (Figure 4B & Table S2). These patterns show that OC in fluvial and eolian systems is selectively preserved by minerals as a result of intensive erosion, degradation, oxidation, and microbial respiration.

^{14}C age patterns to show mineral protection without microbial respiration

Rock varnish on limestone bedrock surface over karst landscape in subtropical SW China is an OC-rich veneer, comprising approximately 13%-26% and 29%-49% OC in two of our study areas, formed by fixation of OC compounds by Fe-Mn minerals (Figure 1C). As erosion removes soil mass, bedrock becomes exposed, and varnish layers developed on newly exposed bedrock surfaces. In this context, the thermally labile-recalcitrant fractions of rock varnish OC yield AMS ^{14}C dates that are older than those of the thermally stable fractions (Figure 4C & Table S3). Similarly, our previously obtained thermally labile-recalcitrant and thermally stable OC fractions from flood-induced sediments in caves within the warm-humid karst region of the central United States yielded identical ^{14}C dates[34] with similar trends (Figure 4D & Table S3). In both cases, the results deviate from those expected on the basis of the Arrhenius equation. These reversed or identical age patterns imply OC cycling dynamics in which OC compounds are protected from microbial respiration, weathering, and oxidation by natural shielding mechanisms (Figures 4C-D).

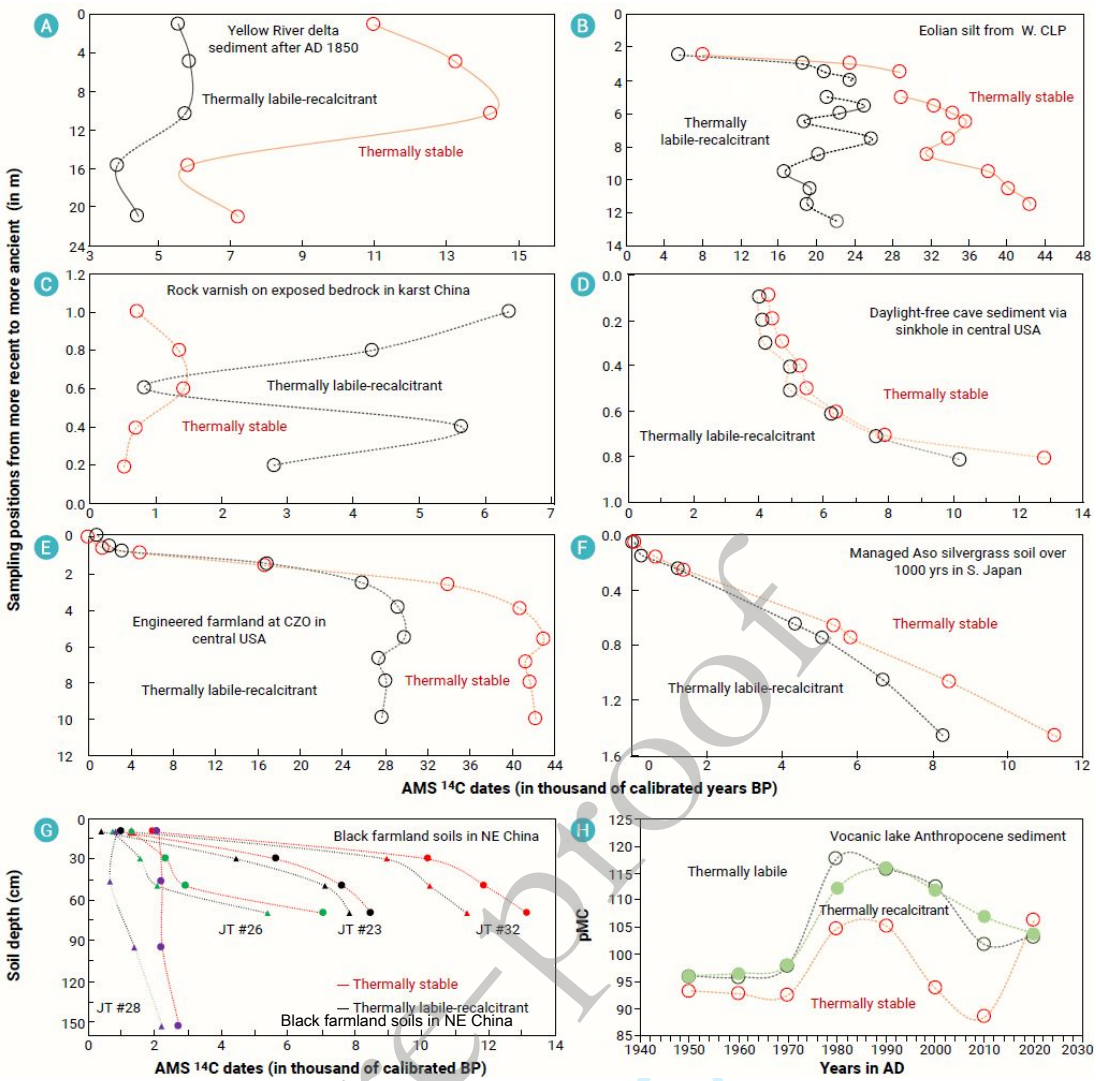

Figure 4. **AMS ^{14}C age patterns of OC fraction cycling dynamics. A-B**. Consistent with the first-order rate assumption of the Arrhenius equation, thermally stable and labile-recalcitrant OC fractions yield constant older-younger AMS ^{14}C age patterns indicating selective preservation dynamics. **C-D**. Contradicting the first-order reaction rate, as expressed by an Arrhenius relationship, thermally stable and labile-recalcitrant OC fractions yield reversed younger-to-older or identical AMS ^{14}C age patterns indicating protective dynamics; For sampling rock varnish: exposed bedrock base is set as 0 (m). **E-F**. Identically modern-aged AMS ^{14}C dates of thermally stable and labile-recalcitrant OC fractions in upper profiles and older-younger age offset patterns in lower profiles, revealing transition from unprotected to stabilized OC pools. **G**. AMS ^{14}C dates of thermally labile-recalcitrant and stable fractions exhibit closely-spaced younger-to-older age offsets up to 10000 years in JT #32 due to erosion and remains unchanged in JT #28 indicating OC accumulation. **H**. pMC of thermally labile, recalcitrant, and stable OC fractions captures atmospheric ^{14}C/^{12}C changes since AD 1950 with constant younger-to-older age offset. Reversely. in AD 2010 and 2020, thermally labile fraction is ~5% lower and stable fraction is ~2.5% higher than other fractions.

^{14}C age patterns to show unprotected to organo-mineral transition

Modern and identical AMS ^{14}C dates for thermally stable and labile-recalcitrant organic carbon fractions near the surface, along with consistent younger-to-older age

patterns in lower critical zone profiles at the central United States[36] and silvergrass farmland in southern Japan[48], reveal distinct pools of unprotected and mineral-protected OC (Figures 4E-F & Table S4). Ecosystems with high biological productivity produce abundant unprotected SOC in near-surface horizons, where no measurable microbial respiration-induced age offset is observed between thermally sensitive OC fractions. As unprotected OC is progressively fixed by minerals at greater soil depths, age offsets between thermally sensitive fractions emerge, consistent with recycling of carbon. These ^{14}C age pattern shifts provide valuable insights into how unprotected organic carbon progressively migrates into organo-mineral associations across different ecosystems.

^{14}C age patterns to show OC dynamics in heavily cultivated soils

Black mollisol farmland in cool-humid NE China is heavily cultivated (Figure 2A). AMS ^{14}C dates of thermally labile-recalcitrant and stable OC fractions of four mollisol profiles in the Jiutai (JT) City District, Jilin Province, show closely spaced non-modern younger-to-older age patterns (Figure 4G & Table S5). Among four farmlands, AMS ^{14}C age patterns of JT #32 and #23 profiles reveal severe OC erosion, indicated by large age increases over intervals of only 10 cm, while profile JT #28 shows remarkable OC accumulation, evidenced by consistent ages throughout the most soil profile (Figure 4G).

^{14}C age patterns to show OC dynamics in high-closure lacustrine

A high-closure volcanic lake sediment (Figure 2B), located adjacent to the black farmland profiles in the cool-humid climatic zone, captures Anthropocene sedimentation history spanning AD 1950–2020 by varve counting and measurements of ^{137}Cs, $^{240/239}Pu$, and ^{129}I anthropogenic radioisotope between 0 and 9 cm depths[49–51]. The depth of 0-1 cm depth is modeled as AD 2020, while depth of 8.3 cm was modeled

as AD 1950. [49–51] The pMC values of thermally labile, recalcitrant, and stable OC fractions reflect atmospheric $^{14}C/^{12}C$ changes since the beginning of the Anthropocene Epoch, with the exception of AD 2010 ± 3 years and AD 2020 ± 3 years. Specifically, in AD 2010, the pMC value of the thermally labile fraction is reversed approximately 5% lower (older) than that of the thermally recalcitrant fraction. In AD 2020, the pMC value of the thermally stable fraction is reversed approximately 2.5% higher (younger) than either the thermally labile or recalcitrant fractions (Figure 4H & Table S6). These results demonstrate that high-resolution AMS ^{14}C dates and tracers of OC compounds in this drainage-free lake within the cool-humid forest ecosystem reveal how selective preservation mechanisms mainly stabilize different OC fractions over time.

DISCUSSION

To increase the ability of terrestrial ecosystems to store carbon and to sequester atmospheric CO_2 for climate change mitigation, both the long-term stability and high input of biosphere OC are equally important. To date, however, no numerical models have succeeded in predicting total SOC stability and turnover times,[7–8] and current geochemical methods remain marginal—or are even incapable of verifying—different OC preservation mechanisms.[5] Our technology, which partitions thermally labile-recalcitrant and stable OC fractions for AMS ^{14}C dating while providing biochemical characterization and source origin information, offers benchmarks for verifying proposed selective and protective OC preservation mechanisms. We find that consistent with the first-order rate assumption of the Arrhenius equation, thermally labile-recalcitrant and stable OC fractions yield constantly younger-to-older AMS ^{14}C age patterns, verifying a selective preservation mechanism by minerals. This age pattern captures configuration of OC fractions following long and intense microbial respiration. In one case, AMS ^{14}C age offsets spanning 10^4-year ranges in the Yellow River deltaic

fluvial and western Chinese loessland eolian silt profiles reveal that intensively respired OC from erosion areas, transported via eolian and fluvial processes, is selectively preserved to form stabilized OC-mineral associations in the deposition areas. In the other case, age offsets spanning $10^{2\text{-}3}$-year ranges in farmland and high-closure lacustrine sediments indicate in-situ selective preservation mechanisms driven by local microbial respiration.

A striking observation is that thermally stable and labile-recalcitrant OC fractions yield random age patterns, including reversed younger-to-older and/or identical AMS ^{14}C ages. These patterns reflect the configuration of terrestrial OC compounds with variable or identical origins and without strong signals of microbial respiration. Such age patterns provide potential benchmarks for verifying OC protective mechanisms in terrestrial organo-mineral associations. In addition, in high-OC-stock ecosystems, both thermally labile-recalcitrant and stable fractions yield modern age signals in the rhizosphere and exhibit progressively larger younger-to-older age offsets toward deeper zones. These age patterns capture the configuration of terrestrial OC fractions transitioning from unprotected biopolymers to persistent organo-mineral associations, demonstrating this important transformative process.

Before asserting that pyrolysis-combustion for AMS ^{14}C dating technology offers the potential to verify OC cycling mechanisms currently only hypothesized in modeling studies, we conducted three experiments to reconcile uncertainties and concerns associated with this approach. The first experiment mixed two end-member reference materials composed predominantly of labile-recalcitrant or stable OC compounds with different ages to test whether their AMS ^{14}C dates are regulated by the dominant OC fractions. We mixed an older international reference materials of humic acid crystals with overwhelmingly dominant thermally stable fractions and

international modern oxalic acid reference material with overwhelmingly dominant thermally labile compounds. We also mixed an older animal protein residue with dominant thermally labile-recalcitrant compounds and younger international reference material of charcoal with dominant thermally stable compounds. AMS ^{14}C dating results confirm that the pyrolysis-combustion technology partitions labile-recalcitrant and stable OC fractions reasonably well, without significant transformation of labile-recalcitrant into stable OC fractions, at least in these two end-member tests (Table 1 & Figure 5).

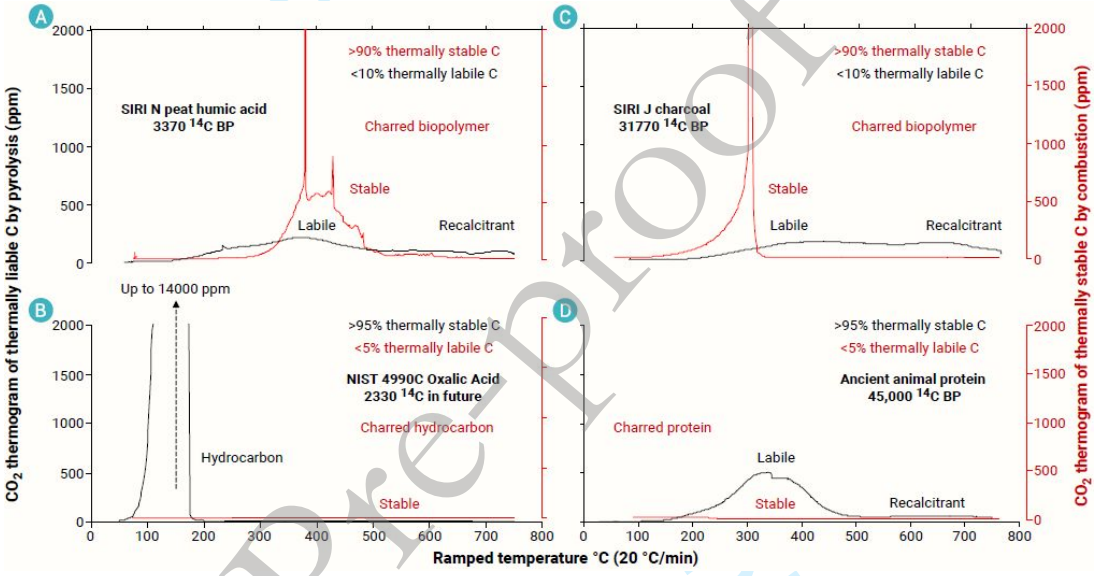

Figure 5. **Thermographs of CO_2 of OC materials with different ages for two end-member mixture test A**. The 3370-year-old SIRI N peat humic acid yields overwhelmed stable (red) with small amount labile-recalcitrant (black) fractions. **B**. Modern oxalic acid standard of NIST 4990C yields overwhelmed labile fractions with trace amount recalcitrant and stable OC compounds. **A** and **B** are mixed for AMS ^{14}C dating test by using pyrolysis-combustion technology. **C**. The 31770-year-old SIRI J charcoal yields large amount stable and small amount labile-recalcitrant compounds. **D**. The 45000-year-old animal protein from a paleolithic site yields dominant amount labile and small amount recalcitrant and stable organics. **C** and **D** are mixed for test.

Table 1. AMS ^{14}C dates of two end member mixture test.

Sample#	Wt (mg)	^{14}C age BP	± 1σ	IntCal20 BP	± 2σ
SIRI N humic acid	4.19	3370	25	3605	100
NIST OX II acid	3.83	-2330	20	-	
SIRI J charcoal	2.40	31770	1065	36285	2420
Old animal protein	15.9	45000	1800	47570	3875
Thermally labile-recalcitrant of SIRI N + OX II		-130	40	-	
Thermally stable of SIRI N + OX II		3360	40	3590	105
Thermally labile-recalcitrant of SIRI J + animal protein		41100	350	44085	670

Thermally stable of SIRI J + animal protein	38430	260	42415	220

The second experiment involved analyzing CO_2 thermograms from pyrolysis and combustion over a ramped temperature range of 40–750 °C, recorded by our IRGA device. We observed that the widely used Rock-Eval analysis for characterizing thermally sensitive OC fractions[38–41] shares fundamental principles with our pyrolysis-combustion technology for AMS ^{14}C dating. [3-4]

We directly correlate our thermally labile fractions (< 450°C) and thermally recalcitrant OC fractions (> 450°C) to Rock-Eval's hydrocarbon-biopolymer and biopolymer fractions, respectively, and our thermally stable OC fractions to Rock-Eval's biopolymer-geopolymer fractions.[42–45] Specifically, two CO_2 thermograms were obtained from rock varnish OC samples: one sample exhibited the normal age pattern, with labile-recalcitrant OC fractions younger and stable OC fractions older over timescales of 10^2 years, while the other showed a reversed pattern, with labile-recalcitrant OC fractions older and stable OC fractions younger over timescales of 10^3 years (Figure 4C). The CO_2 thermograms of rock varnish veneer OC samples exhibiting the normal age pattern reveal that thermally stable compounds contain a significant amount of charred labile-recalcitrant compounds, suggesting in-situ respiration on limited OC sources (Figure 6A). In contrast, the CO_2 thermograms of samples showing reversed age patterns indicate that thermally stable compounds are not charred products of labile-recalcitrant fractions (Figure 6B). In this case,

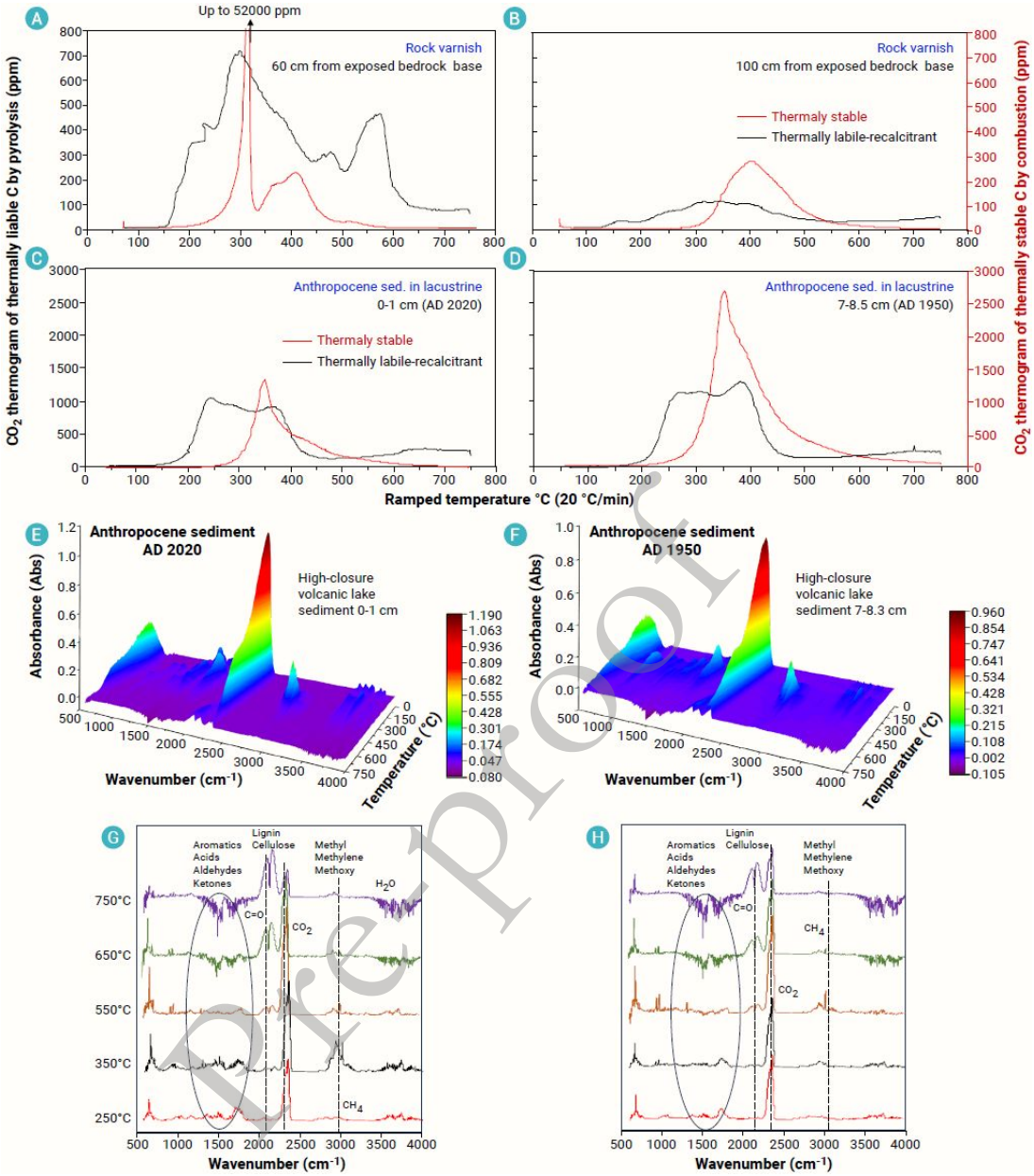

Figure 6. **Origin and evolution of thermally labile-recalcitrant and stable OC compounds by interface of pyrolysis-combustion and online IRGA and FTIR methods**. **A** and **B**. The CO_2 thermograms of rock varnish at 60 and 100 cm above the bedrock base. **C** and **D**. The CO_2 thermograms of Anthropocene samples in 0-1cm and 7-8.5 cm depths. **E** and **F**. Comparation of continuous FTIR spectra of 0-1 and 7-8.3 cm sedimentary samples of the Anthropocene sediments. **G** and **H**. Selected FTIR spectra of 0-1 and 7-8.3 cm sedimentary samples of the Anthropocene sediments at different temperatures.

labile-recalcitrant OC compounds may originate from old hydrocarbons sourced from deep sediments through karst cracks and sinkholes, while stable OC compounds may be derived from younger elemental carbon released by local wood burning. Both older

and younger OC compounds are rapidly fixed by Fe-Mn oxides on the bedrock surface without significant microbial respiration.

Because the CO_2 thermograms of the Anthropocene samples from 0–1 cm (AD 2020) and from 7–8.3 cm (AD 1950) depths in the high-closure lake could not differentiate the origins of labile and stable OC (Figures 6C-D), we conducted a third experiment. In this case, we analyzed gas-phase FTIR spectra to identify OC functional groups[52-54] that contribute to the higher pMC value (younger) in thermally stable than in labile and recalcitrant OC fractions. Comparation of selected FTIR spectra of 0-1 (AD 2020) and 7-8.3 cm (AD 1950) sedimentary samples show that pyrolysis products vary largely in similar absorbance bands with variable intensities in different temperature ranges (Figures 6E-F). Absorbance bands in 1900-1450 cm^{-1}, mainly for the stretching vibrations of aromatics, acids, aldehydes and ketones, [52-53] are observed with the greater intensities in 0-1 cm sediment especially in 250°C -550°C ranges, suggesting increasing aromaticity in AD 2020 sample (Figures 6E-F). Absorbance bands in 2000–2250 cm^{-1} indicate presence of CO, resulted from pyrolysis degradation of lignocellulosic structures, [52-53] and intensity is lower in 250-550 and higher in 650-750 °C (Figures. 6G-H). Finally, the absorbance bands at the region in 2850–3030 cm^{-1} reveal hydrocarbon gas consisting mainly of CH_4 due to small amount of methyl, methylene, and methoxy group decomposition (Figures 6G-H).[52,54] Results of increasing aromaticity and high-temperature lignocellulose products in AD 2020 sample reveal that perhaps burning of forest wood with 30-50 years' life span produces aerosols causing higher pMC values in the thermally stable OC compounds (Figure 4H).

CONCLUSION

We conclude that this novel technology, combined with Rock-Eval and FTIR spectra analyses, provides high precision results for verifying terrestrial OC

preservation mechanisms that are currently known only from modeling simulations. In fluvial, eolian, and farmland ecosystems, thermally labile-recalcitrant and stable OC fractions exhibit constantly younger-to-older AMS ^{14}C age patterns across the 10^2–10^4-year range, exemplifying the selective preservation of OC compounds by minerals under microbial respiration. In contrast, the same OC fractions from rock varnish and flood sediments in karst cracks and sinkholes display reversely older-to-younger or identical ^{14}C age patterns, illustrating the protection of OC compounds by minerals in the absence of intensive respiration. In high OC-stock ecosystems, these fractions yield uniformly modern ages in rhizosphere but show younger-to-older age patterns in deeper zones, reflecting the dynamics of naturally unprotected bio-OC progressively transforms into OC-mineral associations. The CO_2 thermograms obtained via the IRGA and OC functional groups by FTIR analysis provide biochemical evidence to assess origin of terrestrial OC compounds, thereby improving our understanding of their age patterns.

These results also show that OC decay dynamics by using this technology follows the first-order kinetics in the activation energy distribution that is independent from experimental conditions. Because the Arrhenius equation ($k = Ae^{-Ea/RT}$) that considers the pre-exponential factor or the Arrhenius factor (A) and the molar activation energy (Ea) to be temperature independent constants[55] applies to our works, this updated technology could provide reliable Ea values for variable OC thermal fractions. The molar activation energy (Ea) is a proxy for carbon bond strength of OC components, which regulate their stability in the terrestrial ecosystems.[5, 21] In future studies, AMS ^{14}C age patterns among thermally sensitive OC fractions can be further compared with the Ea values not only to identify types but also to quantify terrestrial OC cycling dynamics.

REFERENCES

1. Friedlingstein P., O'Sullivan M., Jones, W., et al. (2023). Global carbon budget 2023. *Earth Syst. Sci. Data* **15**:5301-5369. DOI: 10.5194/essd-15-5301-2023
2. Davidson E.A. and Janssens I.A. (2006). Temperature sensitivity of soil carbon decomposition and feedbacks to climate change. *Nature* **440**:165-173. DOI:10.1038/nature04514
3. Crowther T.W., Todd-Brown K.E.O., Rowe C.W. et al. (2016). Quantifying global soil carbon losses in response to warming. *Nature* **540**: 104-108. DOI:10.1038/s41467-022-33278-w
4. Wang M.M., Guo X.W., Zhang, S. et al. (2022). Global soil profiles indicate depth-dependent soil carbon losses under a warming climate. *Nat. Commun*. **13**: 5514. DOI:10.1038/s41467-022-33278-w
5. Hemingway J.D., Rothman D.H., Grant K.E. et al. (2019). Mineral protection regulates long-term global preservation of natural organic carbon. *Nature* **570**: 228-231. DOI:10.1038/s41586-019-1280-6
6. Schmidt M.W.I., Torn M.S., Abiven S. et al. (2011). Persistence of soil organic matter as an ecosystem property. *Nature* **478**: 49-56. DOI:10.1038/nature10386
7. Kleber M.K., Bourg I.C., Coward E.K. et al. (2021). Dynamics interactions at the mineral-organic matter interface. *Nature Reviews Earth & Environment* **2**: 403-421.
8. Moore O.W., Curti L., Woulds C. et al. (2023). Long-term organic carbon preservation enhanced by iron and manganese. *Nature* **621**: 312-317. DOI:10.1038/s41586-023-06325-9
9. Leinweber P. and Schulten H.R. (1999). Advances in analytical pyrolysis of soil organic matter. *J. Anal. Appl. Pyrolysis* **49**: 359–383. DOI: 10.1016/S0165-2370(98)00082-5
10. Plante A.F., Fernández J.M. and Leifeld J. (2009). Application of thermal analysis techniques in soil science. *Geoderma*:**153**, 1–10. DOI: 10.1016/j.geoderma.2009.08.016
11. Kleber M. (2010). What is recalcitrant soil organic matter? *Environ. Chem*. **7:** 320-332. DOI:10.1071/EN10006
12. Davidson E.A. and Janssens I.A. (2006). Temperature sensitivity of soil carbon decomposition and feedbacks to climate change. *Nature* **440**: 165. DOI:10.1038/NATURE04514
13. Bosatta E. and Agren G.I. (1999). Soil organic matter quality interpreted thermodynamically. *Soil Biol. Biochem*. **31**:1889. DOI:10.1016/S0038- 0717(99)00105-4
14. Fierer N., Craine J.M. and McLauchlan K. (2005). Litter quality and the temperature sensitivity of decomposition. *Ecology* **86**:320. DOI:10.1890/04-1254
15. Conant R.T., Drijber R.A. and Haddix M.L. (2008). Sensitivity of organic matter decomposition to warming varies with its quality. *Glob. Change Biol*. **14**: 868. DOI:10.1111/J.1365-2486.2008.01541. X
16. Feng X.J. and Simpson M.J. (2008). Temperature responses of individual soil organic matter components. *J. Geophys. Res*. 113, G03036 (2008). doi:10.1029/2008JG000743
17. Zhang Y.S., Galy V., Yu M. et al. (2022). Terrestrial organic carbon age and creativity in the Yellow River fueling efficient preservation in marine sediments. *Earth and Planetary Science Letters* **585**: 117515. DOI:10.1016/j.epsl.2022.117515
18. Bolan N. Kumar M., Gupta J et al. (2026). Sources, distribution, stability and management of deep soil carbon in agricultural systems. *Carbon Research* **5**:30. DOI:10.1007/s44246-026-00270-8
19. Schulten HR. and Schnitzer M. (1997). Chemical model structures for soil organic matter and soils. *Soil Sci.* **162**: 115. DOI:10.1097/ 00010694-199702000-00005
20. Swift R. (1999). Macromolecular properties of soil humic substances: fact, fiction and opinion. *Soil Sci*. **164**: 790. DOI:10.1097/00010694- 199911000-00003

21. Hemingway J.D., Rothman D.H., Rosengard S.Z. et al. (2017). Technical note: an inverse method to relate organic carbon reactivity to isotope composition from serial oxidation. *Biogeosciences* **14**: 5099–5114. DOI: 10.5194/bg-14-5099-2017
22. Gutfreund H. (1995). Kinetics for the Life Sciences (Cambridge University Press: Cambridge, UK). https://doi.org/10.1017/CBO9780511626203
23. Fierer N., Colman B.P., Schimel J.P. et al. (2006). Predicting the temperature dependence of microbial respiration in soil: a continental-scale analysis. *Global Biogeochem. Cy*. **20**: GB3026. DOI:10.1029/2005GB002644
24. Keiluweit M., Nico P.S. and Johnson M.G. (2010). Dynamic molecular structure of plant biomass-derived black carbon (biochar). *Environ. Sci. Technol*. **44**: 1247-1253. DOI: 10.1021/es9031419
25. Williams E.K., Rosenheim B.E. and NcNichol A.P. (2014). Charring and non-additive chemical reactions during ramped pyrolysis: Applications to the characterization of sedimentary and soil organic material. *Organic Geochemistry* **77**: 106-114. DOI: 10.1016/j.orggeochem.2014.10.006
26. Rosenheim B.E., Day M.B. and Domack E. (2008). Antarctic sediment chronology by programmed-temperature pyryolysis: Methodology and data treatment. *Geochemistry, Geophysics, Geosystems* **9**: Q04005. DOI:10.1029/2007GC001816
27. Ginnane C.E., Turnbull J.C., Naeher S. et al. (2024). Advancing Antarctic sediment chronology through combined ramped pyrolysis oxidation and pyrolysis-GC-MS. *Radiocarbon* **66**. DOI:10.1017/RDC.2023.116 (2024)
28. Zigah P.K., Minor E.C., McNIchol A.P. et al. (2017). Constraining the sources and cycling of dissolved organic carbon in a large oligotrophic lake using radiocarbon analyses. *Geochim. Cosmochim. Acta* **208**: 102-118. DOI: 10.1016/j.gca.2017.03.021
29. Hedges J. (1978). The formation and clay mineral reactions of melanoidins. *Geochim. Cosmochim. Acta* **42**, 69–76. DOI: 10.1016/0016-7037(78)90218-1
30. Piccolo A. (2001). The supramolecular structure of humic substances. *Soil Sci*. **166**: 810. DOI:10.1097/00010694-200111000-00007
31. Sutton R. and Sposito G. (2005). Molecular structure in soil humic substances: the new view. *Environ. Sci. Technol*. **39**: 9009. DOI:10.1021/ ES050778Q
32. Marschner B., Brodowski S., Dreves A. et al. (2008). How relevant is recalcitrance for the stabilization of organic matter in soils? *J. Plant Nutr. Soil Sci*. **171**: 91–110. DOI.org/10.1002/jpln.200700049
33. Kleber M. and Johnson M.G. (2010). Advances in understanding the molecular structure of soil organic matter: implications for interactions in the environment. *Adv. Agron*. **106**: 77–142. DOI:10.1016/S0065-2113(10)06003-7
34. Wang H., Hackley K.C., Panno S.V. et al. (2003). Pyrolysis combustion 14C dating of soil organic matter. *Quaternary Research* **60**: 348-355. DOI:10.1016/j.yqres.2003.07.004
35. Wang H., Ambrose S., Headman K. et al. (2010). AMS 14C dating of human bones using sequential pyrolysis and combustion of collagen. *Radiocarbon* **52**: 157-163. DOI: 10.1017/S0033822200045100.
36. Wang H., Stumpf A.J. and Kumar P. (2018). Labile and inert carbon cycling dynamics in the Critical Zone Observatory in Illinois, USA. *Radiocarbon* **60**: 989-999. DOI:10.1017/RDC.2018.31
37. Cheng P., Zhou W.J., Wang H. et al. (2013). 14C dating of soil organic carbon (SOC) in loess-paleosol using sequential pyrolysis and accelerator mass spectrometry (AMS). *Radiocarbon* **55**: 563-570. DOI: 10.1017/S0033822200057696
38. Disnar J.R., Guillet B., Keravis D. et al. (2003). Soil organic matter (SOM) characterization by Rock-Eval pyrolysis: scope and limitations. *Organic Geochemistry* **34**: 327-343. DOI: 10.1016/S0146-6380(02)00239-5
39. Baudin F., Disnar J.R., Aboussou A. et al. (2015). Guidelines for Rock-Eval analysis of recent marine sediments. *Organic Geochemistry* **86**: 71-80. DOI:10.1016/j.orggeochem.2015.06.009

40. Sebag D., Verrecchia E.P., Cecillon L. et al. (2016). Dynamics of soil organic matter based on new Rock-Eval indices. *Geoderma* **284**: 185-203. DOI: 10.1016/j.geoderma.2016.08.025

41. Lamoureux-Var V., Bouton N., Espitalie J. et al. (2023). Chapter 2. Principles and methods. In The Rock-Eval Method ed. by Baudin, F. pp. 11-27. ISTE London, UK and Wiley Hoboken NJ USA (2023). DOI: 10.1002/9781394256235

42. Albrecht R., Sebag D. and Verrecchia E. (2015). Organic matter decomposition: bridging the gap between Rock–Eval pyrolysis and chemical characterization (CPMAS 13C NMR). *Biogeochemistry* **122**: 101–111. DOI:10.1007/s10533-014-0033-8

43. Barré P., Plante A.F., Cécillon L. et al. (2016). The energetic and chemical signatures of persistent soil organic matter. *Biogeochemistry* **130**: 1–12. DOI:10.1007/s10533-016-0246-0

44. Carrie J., Sanei H. and Stern G. (2012). Standardization of Rock–Eval pyrolysis for the analysis of recent sediments and soils, *Organic Geochemistry* **46:** 38–53. DOI:10.1016/j.orggeochem.2012.01.011

45. Cécillon L., Baudin F., Chenu C. et al. (2018). A model based on Rock-Eval thermal analysis to quantify the size of the centennially persistent organic carbon pool in temperate soils. *Soil Biology and Biochemistry* **117**, 117-124. DOI: 10.5194/bg-15-2835-2018

46. Pang J.Z. and Si S.H. (1979). The estuary changes of Huanghe River I. Changes in modern time. *Oceanologia et Liminologia Sinica* **10**: 136-141.

47. Pang J.Z. and Jiang M.X. (2003). On the evolution of the Yellow River estuary (Part II). *Transactions of Oceanology and Limnology* **4**: 1-13. DOI: 1003-6482(2003)04-0001-13

48. Howlett D.S., Toma Y., Wang H. et al. (2013). Soil carbon source and accumulation over 12,000 years in a semi-natural Miscanthus sinensis grassland in southern Japan. *Catena* **104:** 127–135.DOI: 10.1016/j.catena.2012.11.002

49 Chu G., Gu Z., Xu B. et al. (2005). Varve chronology and radiometric dating (137Cs, 210Pb) from the Sihailongwan Maar, Northeastern China (In Chinese with English Abstract). *Quaternary Sciences* **25**: 202–207. http://www.dsjyj.com.cn/en/article/id/dsjyj_9027?viewType=HTML

50. Mingram J., Stebich M., Schettler G. et al. (2018). Millennial-scale East Asian monsoon variability of the last glacial deduced from annually laminated sediments from Lake Sihailongwan, N.E. China. *Quat. Sci. Rev*. **201**: 57–76. DOI: 10.1016/j.quascirev.2018.09.023

51. Han Y.M, An Z.S., Lei D.W. et al. (2023). The Sihailongwan Maar Lake, northeastern China as a candidate global boundary stratotype section and point for the Anthropocene series. *The Anthropocene Review* **1-24**. DOI: 10.1177/20530196231167019

52. Özsin G.and Pütün A.E. (2017). Kinetics and evolved gas analysis for pyrolysis of food processing wastes using TGA/MS/FT-IR. *Waste Manag*. **64**: 315. DOI: 10.1016/j.wasman.2017.03.020

53. Li T.T., Song F.H. and Zhang J. (2020). Pyrolysis characteristics of soil humic substance using TG-FTIR-MS combined with kinetic models. *Science of the total environment* **698:** 134237. DOI: 10.1016/j.scitotenv.2019.134237

54. Ma Z., Chen D., Jie G. et al. (2015). Determination of pyrolysis characteristics and kinetics of palm kernel shell using TGA–FTIR and model-free integral methods. *Energy Convers. Manag*. **89**: 251–259. DOI: https://doi.org/10.1016/j.enconman.2014.09.074

55. Arrhenius S. A. (1889). On the heat of dissociation and the influence of temperature on the degree of dissociation of the electrolytes. *Z. Phys. Chem*. **4**: 96–116. DOI:10.1515/zpch-1889-0408. S2CID 202553486

FUNDING AND ACKNOWLEDGMENTS

This research was supported by NSFC Grant No. 41991253 and 42072206, LSKJ202203301, and NSFC No. U2243208. Authors thank Mr. Bing Li, Zhen Zhang, Dr. Jianghu Lan, and Dr. Deming Lei for field works. We also thank two anonymous reviewers' valuable suggestions and comments. The funders had no role in study design, data collection and analysis, decision to publish, or preparation of the manuscript.

AUTHOR CONTRIBUTIONS

Conceptualization: H WANG, P CHENG, Y YANG, XF LU, YM HAN, XL HOU, L LIU, WJ ZHOU, ZS AN. Methodology: H WANG, YN LIU, GD MING, XF LU, H DU, F XIAN, SY ZHU, YM SUN, TH Liu, XL ZHAO, F XIAN, L LIU, XL HOU. Investigation: H WANG, XF Gao, Y YANG, YN LIU, J CAO, DX LI, KL ZHANG, BS CUI. Visualization: Y YANG, PX SHU, GD MING, H DU, PX SHU. Supervision: H WANG, XF LU, KL ZHANG, BS CUI. Writing—original draft: H WANG, P CHENG, WJ ZHOU, ZS AN. Writing—review & editing: XL HOU, XL ZHAO, WJ ZHOU, ZS AN. All authors contributed to the manuscript and approved the final version.

DECLARATION OF INTERESTS

The authors declare that they have no known competing financial interests or personal relationships that could have appeared to influence the work reported in this paper.

Different pathways control degradation, protection, respiration, and carbon flux

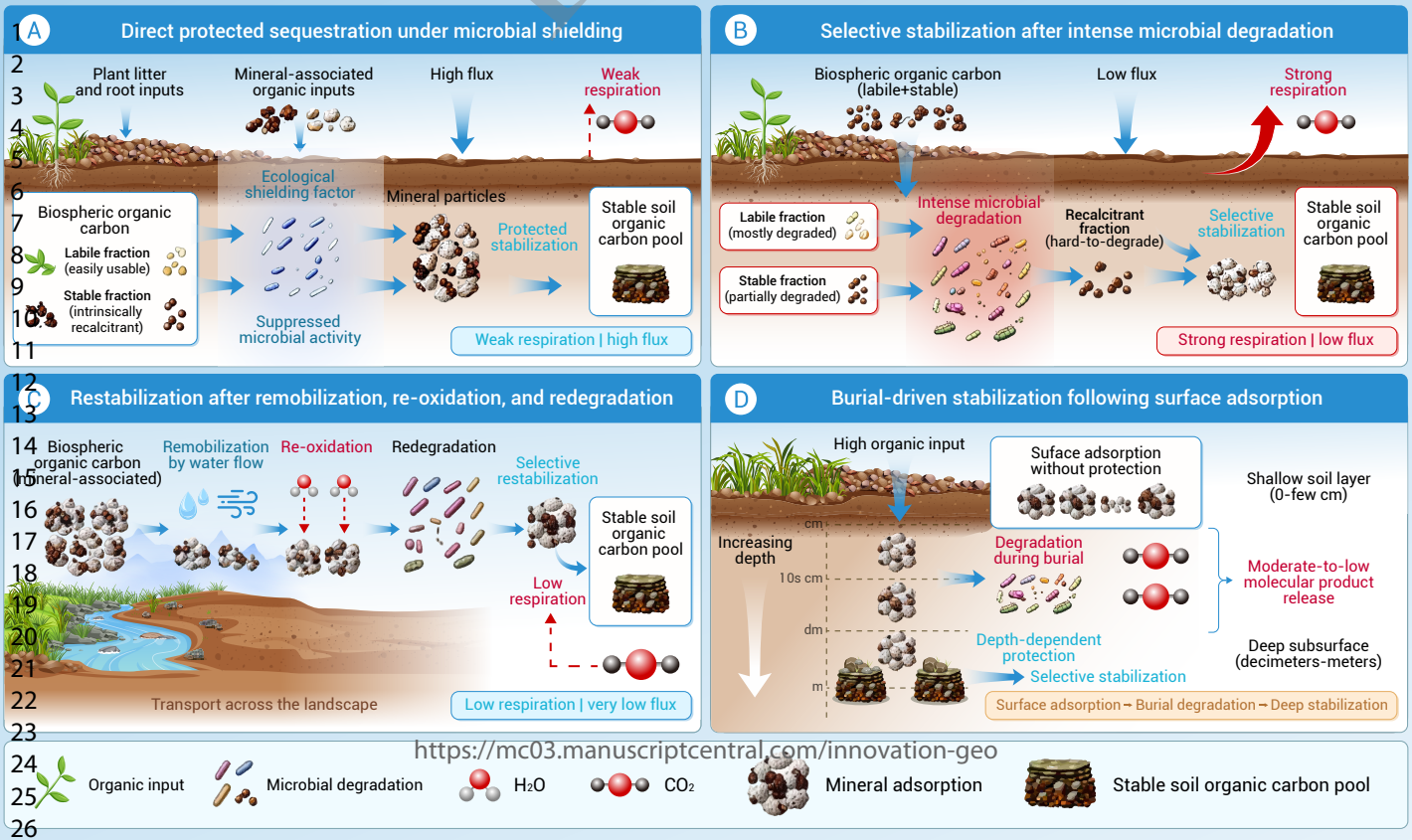


A


B


C1


C2

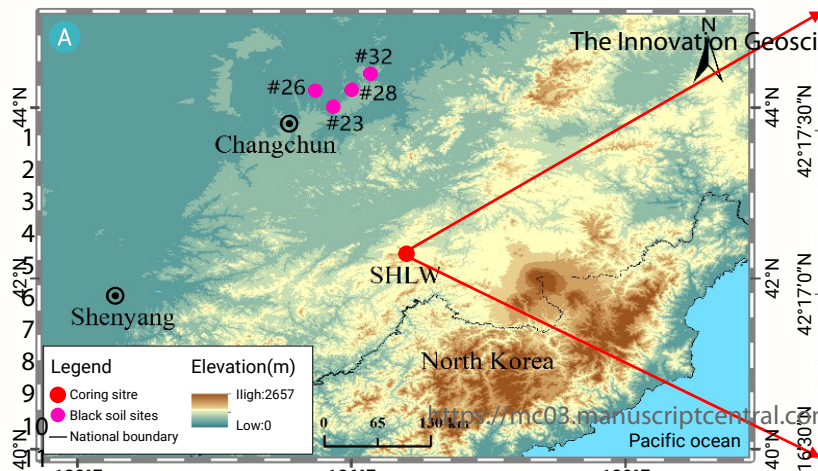

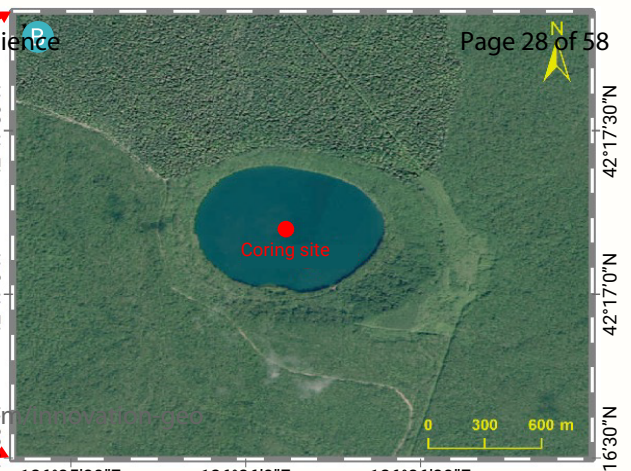

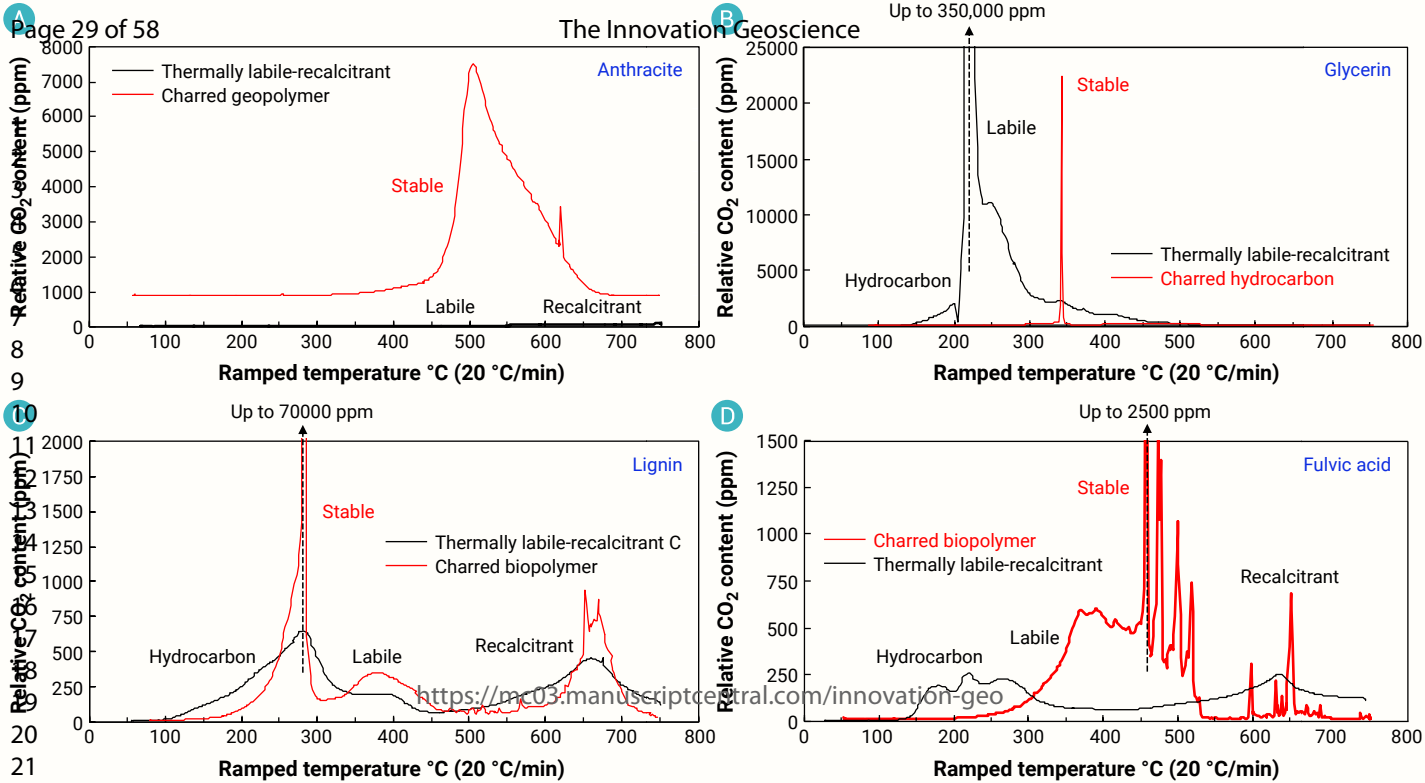

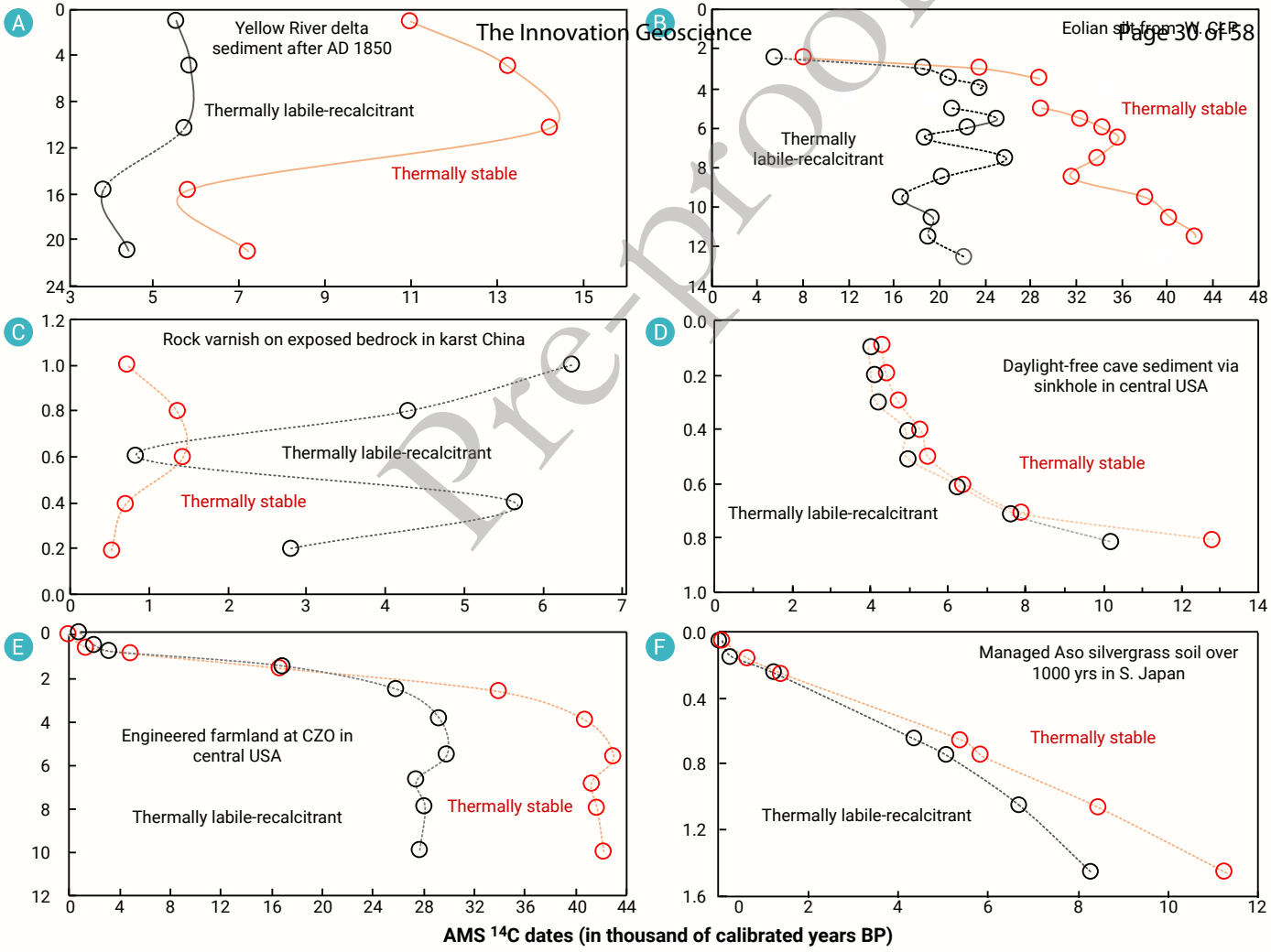

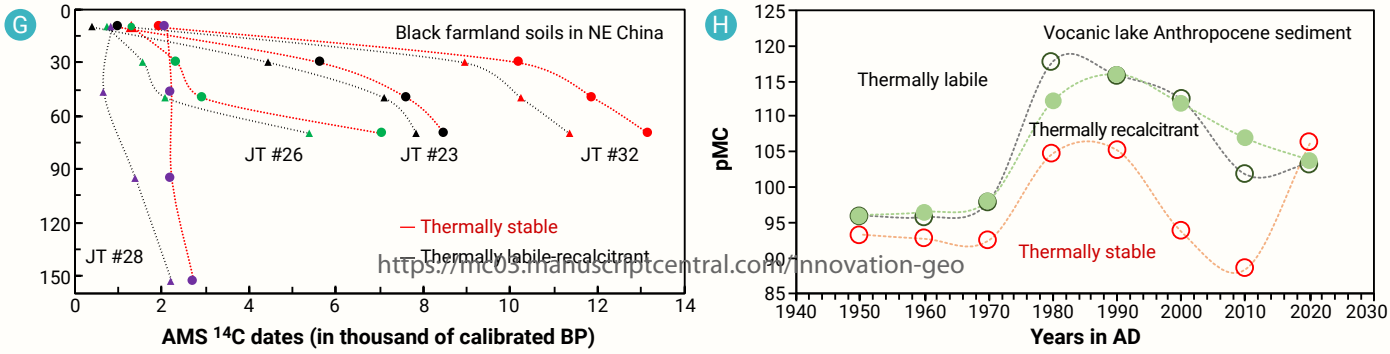

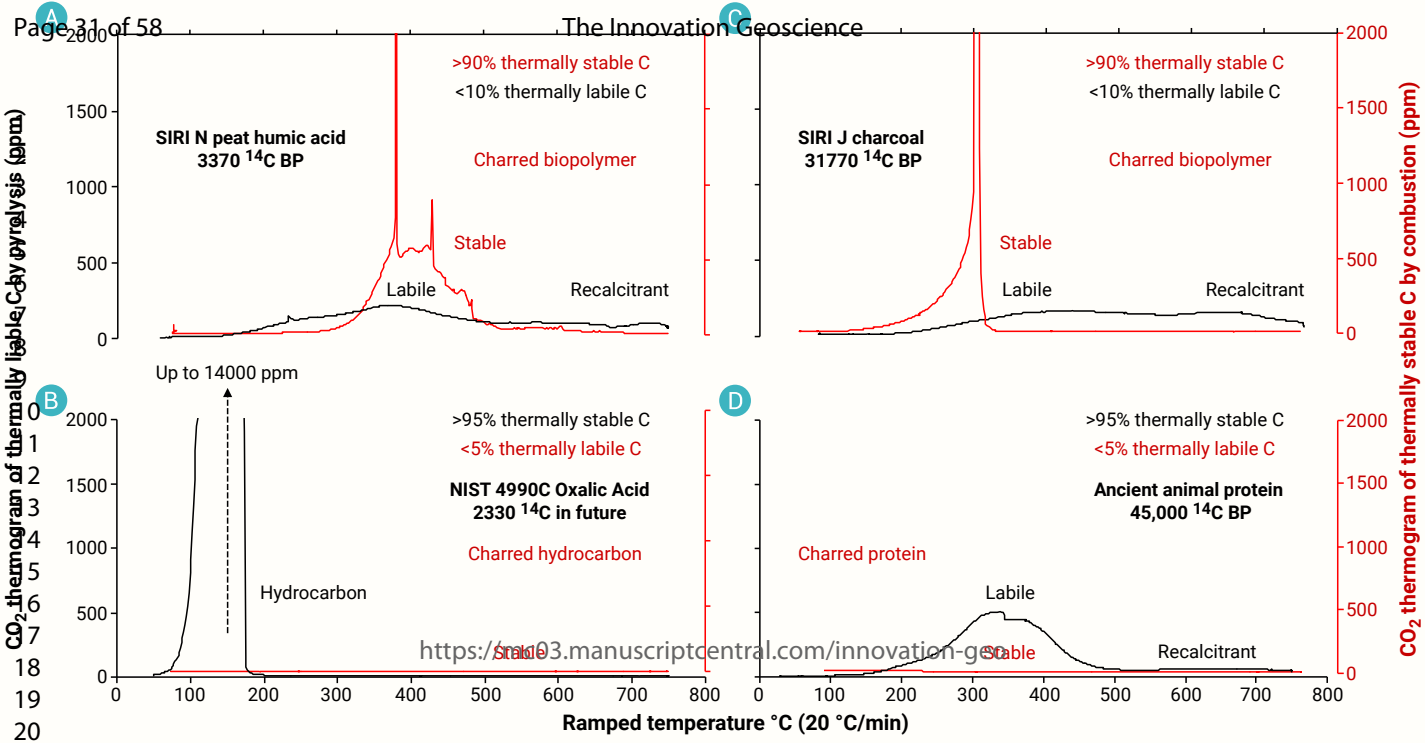

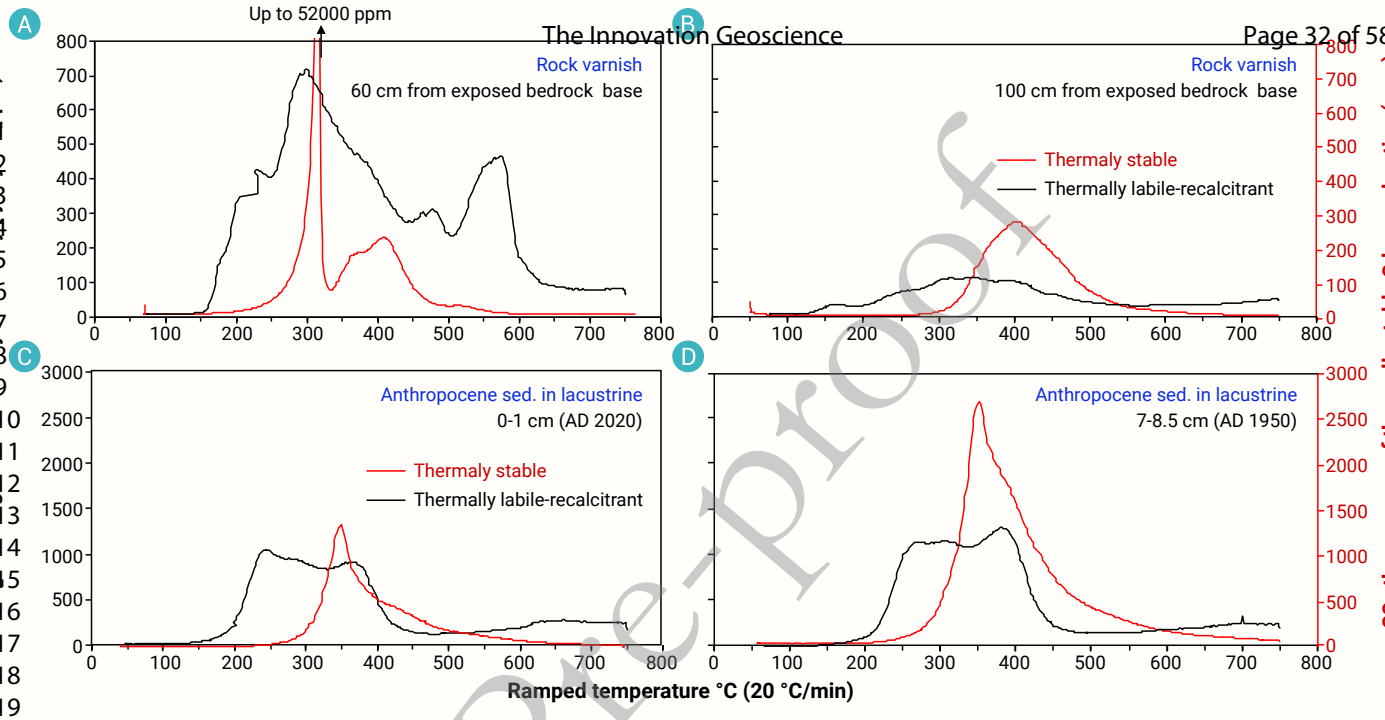

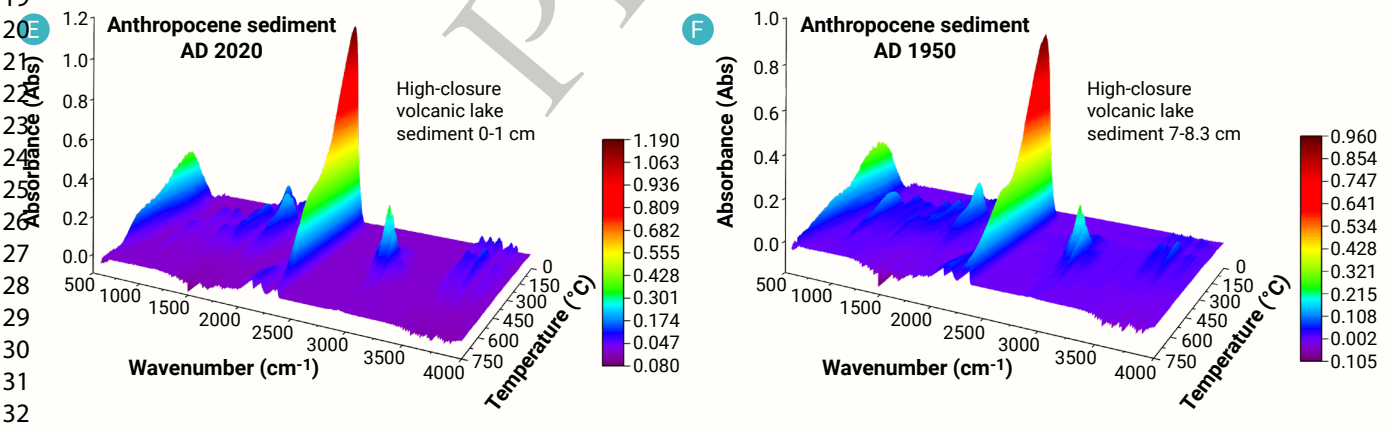

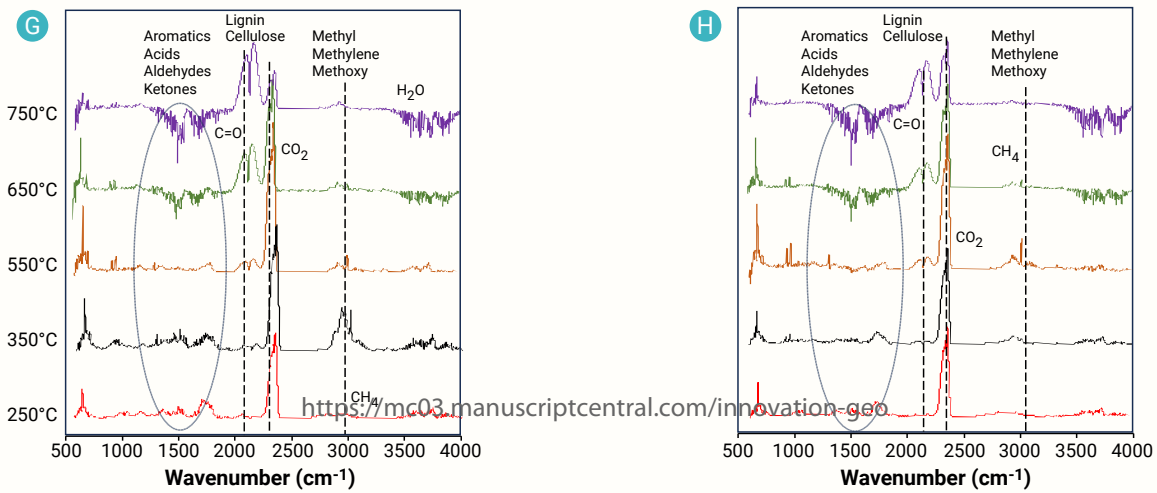

Prof. Hai Cheng July 29, 2026
Editor-in-Chief of the Innovation Geoscience

Dear Professor Cheng
We appreciate reviewer's and editors' suggestions, comments, and helps. Now we submit the final version of the manuscript.

Please find our final version of the manuscript entitled as "AMS ^{14}C dating with biochemical characterization by pyrolysis-combustion and infrared technology reveal terrestrial organic carbon cycling dynamics".

Best Regards.

Professor, Hong Wang

College of Geographical Sciences
Beijing Normal University

hongwang@illinois.edu

AMS ^{14}C dating with characterization by pyrolysis and infrared technology reveal terrestrial organic carbon cycling dynamics

Hong Wang[1,2]*, Xiaofei Gao[1], Yi Yang[1], Peng Cheng[2,6]*, Jia Cao[1], Dongxue Li[3], Peixian Shu[2], Guodong Ming[4], Yingna Liu[1], Keli Zhang[1], Baoshan Cui[3], Yongming Han[2], Xuefeng Lu[2], Hua Du[2], Feng Xian[2], Xiaolin Hou[2], Sanyuan Zhu[5], Yanmin Sun[5], Tianhe Liu[1], Lin liu[1], Xiaolei Zhao[1], Weijian Zhou[2], Zhisheng An[2]

[1] State Key Laboratory of Earth Surface Process and Disaster Rick Reduction, Faculty of Geographical Science, Beijing Normal University, Beijing 100875, China
[2] State Key Laboratory of Loess and Quaternary Geology, , Xi'an 710061, China.
[3] School of Environment, State Key Joint Laboratory of Environmental Simulation and Pollution Control, Beijing Normal University, Beijing 100875, China
[4] Institute of Deep Space Sciences, Deep Space Exploration Laboratory, Hefei 230088, China
[5] State Key Laboratory of Organic Geochemistry, Guangzhou Institute of Geochemistry, Chinese Academy of Sciences, Guangzhou 510640 Guangdong, China.
[6] Institute of Global Environmental Change, Xi'an Jiaotong University, Xi'an, 710049 China
hongwang@bnu.edu.cn
chp@ieecas.cn

Graphical Abstract

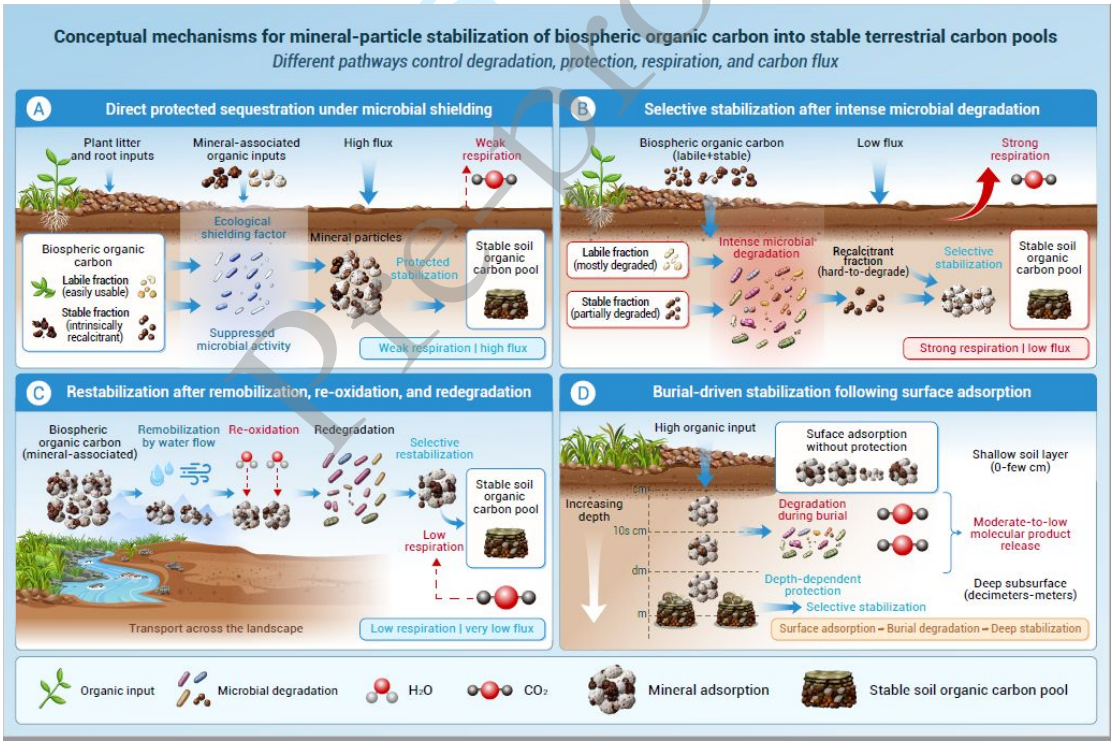

Public summary

- The updated pyrolysis system successfully partitions thermally labile and stable organic carbon fractions.
- Their AMS ^{14}C age patterns demonstrate terrestrial carbon cycling dynamics that are known only in models.
- Their reverse older-younger/identical age patterns exhibit protective preservation under weak respiration.

- Their constant younger-older age patterns exhibit selective preservation under intensive organic degradation.
- Their identical modern to younger-older age patterns across depth reveal organic carbon fixation dynamics.

Key Words:

- Updated pyrolysis technology
- Partition of organic carbon components
- Terrestrial carbon dynamics

ABSTRACT

Terrestrial systems hold twice as much organic carbon (OC) as the atmosphere and vegetation combined. The long-term stability of this carbon pool influences ecological resilience and helps mitigate global climate change. Here, we couple an updated pyrolysis-combustion system with online infrared gas analyzer (IRGA) and Fourier transform infrared spectroscopy (FTIR) to partition OC into thermally labile, recalcitrant, and stable fractions, enabling the analysis of their biochemical structures, origins, and AMS ^{14}C ages. We find that the labile-recalcitrant and stable OC fractions from fluvial, eolian, and farmland ecosystems consistently exhibit younger-to-older age patterns over timescales ranging from 10^2 to 10^4 year. These trends exhibit a first order reaction rate temperature dependance as predicted by Arrhenius equation. This pattern verifies selective preservation of OC compounds by minerals under microbial respiration. In contrast, labile-recalcitrant and stable OC fractions from rock varnish and flooding sediments in karst cracks and sinkholes exhibit reverse (older-younger) or identical age patterns, confirming protection of OC by minerals in the absence of intensive respiration. In high-organic-carbon-stock ecosystems, thermally labile-recalcitrant and stable OC fractions yield identical modern ages in the rhizosphere and younger-to-older age patterns in deeper zones, quantitatively exemplifying the process by which unprotected OC progressively attaches to mineral-associated forms. The CO_2 thermograms from IRGA and the OC functional

groups from FTIR analysis provide biochemical evidence for assessing the origin of terrestrial OC compounds, thereby improving our understanding of their age patterns. We conclude that pyrolysis-combustion technology holds significant potential for revealing the mechanisms underlying terrestrial OC preservation.

INTRODUCTION

Terrestrial systems hold twice as much organic carbon (OC) as found in the atmosphere and vegetation combined[1], influencing food productivity, soil erosion, and climate change mitigation. Microbes and enzymes decompose and respire labile OC compounds (e.g., starch and sugars), into atmosphere[2-4], whereas structurally and energetically recalcitrant OC compounds (e.g., lignin and humin) can survive this process[5]. However, experimental results suggest that chemical structures alone do not regulate soil OC stability, turnover times, or preservation dynamics; rather, ecosystem factors also constrain decomposition rates and protective pathways. For example, soil microaggregates and pore spaces can shield organic carbon from decomposition[5], and the low activity of microbes and enzymes in semi-arid bioclimate zones can slow decomposition rates, whereas high fluxes of dissolved organic carbon can increase OC content in organo-mineral associations within lower soil horizons[6]. To enhance the storage of carbon in terrestrial ecosystems and to sequester atmospheric CO_2 for climate change mitigation, stabilizing biosphere OC is crucial. To date, however, no models have succeeded in predicting soil OC stability and turnover times across different bioclimate zones[7–8].

A key challenge in quantifying the stability and turnover times of different OC components, such as labile and recalcitrant compound groups, for accelerator mass spectrometry (AMS) ^{14}C dating is how to effectively partition these fractions. Wet

chemistry[9–11] and ramped thermal decomposition under low oxygen flow rates[12–17] are commonly used for this purpose. This approach assumes that more intensive procedures, stronger chemical doses, and higher temperature pretreatments yield progressively more recalcitrant organic carbon fractions[18–20]. However, these techniques only marginally or are even incapable of achieving this goal[5, 21–28]. Although humification and mineral protection can produce biochemically stable geopolymers that resist chemical and thermal treatment[7–8, 29], the recycling of stabilized organic carbon can also fragment and simplify these geopolymers, making them susceptible to such treatments[11, 30–31]. Consequently, the "recalcitrant" organic carbon components defined by wet chemistry or low-oxygen combustion become ambiguous, complicating discussions of terrestrial OC stability and cycling dynamics[6, 32–33]. Here, we interfaced an updated pyrolysis-combustion devise, originally for conventional ^{14}C dating[34-37], with an online IRGA and gas-phase FTIR for AMS ^{14}C dating of thermally-sensitive terrestrial OC fractions with biochemical structure information to evaluate the origin and evolution of terrestrial OC compound stability (Figure S1). This pyrolysis-combustion device updates currently the popular apparatus of ramped pyrolysis and low O_2 content oxidation, known as RPO, technology[26-27] in that pyrolysis products (volatile compounds) are purged from the pyrolysis (inner) tube into combustion (outer) tube by Ar gas via an orifice for instant O_2 combustion in outer tube (Figure S1). This design prevents volatile compounds from traveling long distances and interacting with one another. In addition, the higher Ar gas pressure caused by restricted gas flow at the tip of the inner tube further inhibits O_2 backflushing. By partitioning thermally labile-recalcitrant (O_2-free) and stable (with O_2) compounds, this approach generates multiple thermally sensitive CO_2 aliquots for AMS ^{14}C dating analysis (Figure S1). Finally, CO_2 thermograms recorded by the online IRGA and OC functional groups

identified by FTIR spectra provide biochemical structure information for evaluating the origin and evolution of these thermal fractions.

Using this novel technology, we investigated a range of terrestrial systems: current Yellow River deltaic fluvial deposits, western Chinese loessland eolian silt in semi-arid regions, high-closure volcanic lacustrine sediments, black (mollisol) farmland in semi-humid Northeast China, and karst rock varnish veneers in subtropical Southwest China (Figure S2). We further compiled ^{14}C dates from thermally labile-recalcitrant and stable organic carbon fractions derived from flood deposits in caves fed by karst cracks and sinkholes, as well as from a critical zone observatory engineered soil profile in humid central United States and silvergrass farmland soil in subtropical Japan (Figure S2). Together, these data provide benchmarks for verifying terrestrial organic carbon preservation dynamics that have previously been observed only in modeling simulations.

MATERIALS AND METHODS

Sample sites and materials

Terrestrial sediment and soil profiles are collected in Northern Hemisphere middle latitudes for AMS ^{14}C dating on thermally sensitive OC fractions. They include the current Yellow River deltaic floodplain in east coast of China, loess from western Chinese Loess Platea, rock varnishes on newly exposed limestone bedrocks in erosive karst region in SW China, organic-rich mollisol farmland and high-closure lacustrine in NE China. The ^{14}C dates of thermally sensitive OC fractions of flooding sediment sequence in caves in karst region from the central USA, high OC stock grassland farms from S. Japan and engineered soil at the Critical Zone Observatory site from the central USA are compiled for discussion.

Yellow River deltaic sediment: A 21 m long core was collected by percussion corer from current delta near the Bohai Sea coast area at 38°02'N, 118°53' E (Fig. 1A). Subsamples were taken in 0.9-1.0 m, 4.8-4.9 m, 10.2-10.3m, 15.6-15.7 m, 20.9-21m intervals.

Loess profile: A 13m loess section was sampled from western Chinese Loess Plateau in Gansu Province at 36°20'47" N, 107°20'54" E. Subsamples were taken in 0.5 m increments from 3 to 12.5 m depths (Fig. 1B).

Rock varnishes: Rock varnish sequence was scraped in 20 cm increments from 1.2m high limestone rock above sparse bushland surface from the karst Mountain region in the SW China at 25.5 °N, 105.75 °E (Fig. 1C1-C2).

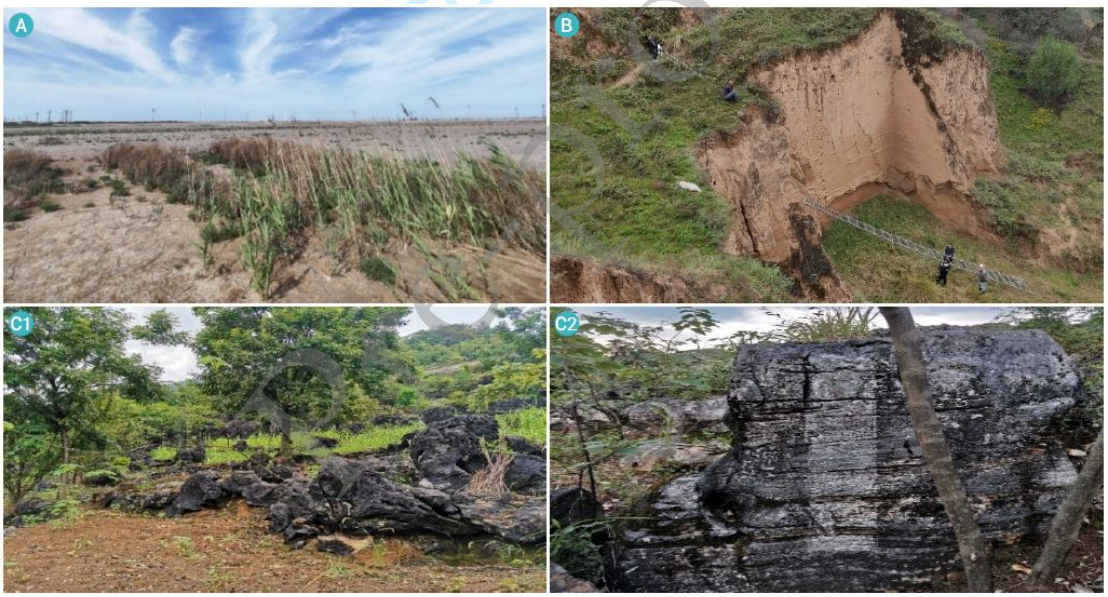

Figure 1. Field views of Yellow River deltaic floodplain, semi-arid western Chinese Loess Plateau, and warm-humid subtropic karst ecosystems. **A**. Current Yellow River delta. **B**. A loess profile from western Chinese Loess Plateau. **C1-2**. Karst geomorphology and rock varnish veneers on bedrock surfaces.

Mollisol farmland soil profiles: A total of 16 mollisol samples from 4 farmland sections in the Jiutai (JT) City areas in NE China by a hand auger. Soil samples were taken in 20 cm increments from the JT#23, #26, and #32 sites, and 0-20, 37-57, 90-100, 144-164 cm depth intervals from the #28 site. They are located at 44°00′00″N, 125°48′

00″E for JT #23; at 44°12′00″N, 125°36′00″E for JT#26; at 44°12′00″N, 126°00′00″E for JT#28; and at 44°24′00″N, 126°12′00″E for JT#32 soil profile (Fig. 2A).

High-closure Mountain Forest volcanic lake sediment: Several frozen cores were collected from the freezing Lake Sihailongwan (SHLW) in NE China (42°17′24″N, 126°35′51″E, Fig. 2B) using a freeze corer (UWITEC GmbH, Austria) in 2022. These cores were immediately stored in a mobile freezer (−36°C) and transported to the Institute of Earth Environment, Chinese Academy of Sciences (IEECAS) in Xi'an for Anthropocene and to Faculty of the Geography at the Beijing Normal University for OC cycling dynamic studies. They have been stored in a freezer under –20°C and subsamples were taken in 1 cm increment from 0 to 8.5 cm depths that spins from AD 1950 to AD 2020.

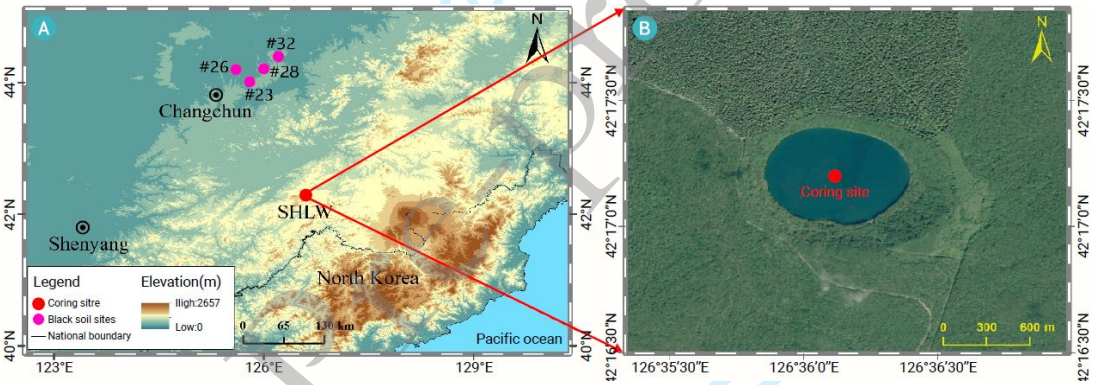

Figure 2. Location of four mollisol farmland sites and the high-closure mountain forest volcanic lake (Lake Sihailongwan, SHLW). **A**. Mollisol farmland selected for carbon cycling studies in Jilin Province, NE China. **B**. High-closure Mountain Forest volcanic lake sediment selected for air-born OC cycling studies.

Experimental analysis

Chemical pretreatment: About 2-5g of soil and sediment or 0.5g of rock varnish samples from different terrestrial ecosystems were pretreated by using hot 2 M HCl at 80 °C for 2 hours, rinsed to neutrality using ultra-pure Mili-Q water, oven-dried at 70 °C overnight.

Thermally sensitive OC fractional characterization: For sediment/soil specimens, about 0.2-0.5g and for rock varnish specimen 0.01-0.02g rock varnish samples were weighted and transferred into the inner pyrolysis quartz tube or a small quartz glass boat in the inner tube (Figure S1A). When combustion furnace reaches to 750 °C, Ar gas is purged into inner tube and O_2 gas is purged into outer quartz tube, and flow-control valve is adjusted to maintain total pressure at 1.5 psi with Ar pressure is slightly greater than O_2 pressure and Ar gas flows at 80ml/min and O_2 flows at 50ml/min. Then, pyrolysis furnace increases temperature from 40 to 750 °C in 35 minutes and ramped rate is ~20 °C/min. The CO_2 thermogram of thermally labile-recalcitrant OC fraction is captured by the online IRGA monitored. After pyrolysis process is completed, the pyrolysis furnace is shut off and wait until it reaches room temperature. This procedure is repeated for thermally stable OC fraction through replacing Ar gas by O_2 in the inner tube. The CO_2 thermogram of thermally stable OC fraction is captured by the online IRGA.

Thermally sensitive OC compounds functional group analysis: Repeat the above procedure with combustion furnace set at 120 °C and no O_2 gas in the outer tube. As pyrolysis furnace ramps up from 40 to 750 °C, the absorbance bands and intensity are recorded by the online FTIR spectroscopy (Figure S1A).

Partition of thermally labile-recalcitrant OC fractions by pyrolysis: 1-3g pretreated and oven dried sediment/soil samples are accurately weighed into the inner tube or 0.05-0.15g of rock varnish samples are weighed in a small quartz boat and insert the boat into the inner tube. After the pyrolysis-combustion system is evacuated to 1-2 mTorr level, the combustion furnace is switched on. When it reaches to 750 °C, the flow-control valve next to the compound gage is shut off and Ar gas is purged into inner tube and O_2 gas is purged into outer tube (Figure S1A). Then, flow-control valve is

adjusted to maintain pressure at 1.5 psi with Ar gas flow rate at 80ml/min and O_2 flow rate at 50ml/min with Ar gas pressure is slightly greater than O_2 pressure. After the pyrolysis furnace reaches to 750 °C and Ar/O_2 air flows are established, the pyrolysis furnace is moved to wrap the sample. Pyrolysis can be conducted at 450 and 750 °C to isolate thermally labile and thermally recalcitrant organic carbon fractions on two peaks of CO_2 thermogram, which together constitute the composite labile-recalcitrant OC fractions of samples on one peak of CO_2 thermogram. Organic compounds that are thermally decomposed from samples are carried by Ar gas from inner to outer tubes via the orifice (Figure S1A), where O_2 gas at consistent 750 °C combusts OC molecules to CO_2. The CO_2 and other combustion gases pass through a cupric oxide and copper/silver furnaces at 750 ºC and a double-loop cold trap for purification, cryogenically collection, measurement, and storage in glass tubes separately.

Partition of thermally stable fraction by combustion of pyrolysis residue: After the pyrolysis, the inner quartz tube is filled with O_2 gas by switching valve to disconnect Ar and connect O_2 supplies to combust the pyrolysis residue at 750ºC with O_2 flows of 80 ml/m in the inner and 50 ml/m in the outer tubes. The inert OC fractional CO_2 with other combustion gases pass through the cupric oxide and copper furnaces at 750 ºC and multiple traps again and is purified cryogenically, measured, and stored in glass tubes separately.

AMS ^{14}C dating: A dozen of reference samples was also processed through the pyrolysis-combustion vacuum system along with studying samples for QA/QC of the dating analysis, e.g., the NIST Oxalic Acid II, the FIRID wood, IAEA C5 (Two Creek Forest) wood, and deadwood blanks were processed at the same time. Aliquot of CO_2 of thermally sensitive OC fractions is used for graphitization using the in-house hydrogen-iron reduction method for AMS ^{14}C dating analysis. The AMS measurement

was conducted at the AMS center in the Institute of the Earth Environment, Chinese Academy of Science, the Guangzhou Institute of Geochemistry, Chinese Academy of Science, and Beijing Normal University (BNU). Results were corrected online for isotopic fractionation according to the conventions of Stuiver and Polach. Sample preparation backgrounds were subtracted based on the measurements from deadwood blanks with pMC (percent of modern carbon) values ranging from 0.25-0.30. All ^{14}C dates were calibrated using the online IntCal20 (Calib 8.2).

RESULTS

Characterization of thermal fractions

The CO_2 thermogram of thermally labile-recalcitrant fractions, defined by pyrolysis, and stable fractions, defined by combustion, can be characterized using Rock-Eval technology[38-41]. The CO_2 fluxes released from OC materials during ramped pyrolysis and combustion in 20 °C/min are comparable to CO_2 thermograms from hydrocarbon decomposition, biopolymer cracking, geopolymer cracking, and charred products obtained by Rock-Eval analysis (Table S1)[42-45]. Here, we propose that thermally labile-recalcitrant OC compounds likely derive from ancient volatile-containing organic carbon (e.g., animal protein residues and petroleum vapors), while thermally stable OC compounds correspond to elemental carbon. For example, the thermally stable fraction is dominant in anthracite, whereas the thermally labile-recalcitrant fraction is overwhelmingly dominant in glycerin, reflecting naturally formed high- and low-molecular-weight OC compounds, respectively (Figs. 3A-3B). Conversely, the CO_2 thermograms of thermally stable fractions from lignin and fulvic materials may reflect charred materials originating from labile-recalcitrant fractions (Figs. 3C-3D). The identification of thermally stable OC compounds as charred

materials, naturally formed elemental carbon, or high molecular weight OC compounds, can be determined through AMS ^{14}C dating analysis. Specifically, overlapping AMS ^{14}C ages between the thermally labile-recalcitrant and stable OC fractions reflect a common origin, otherwise they reflect different origins.

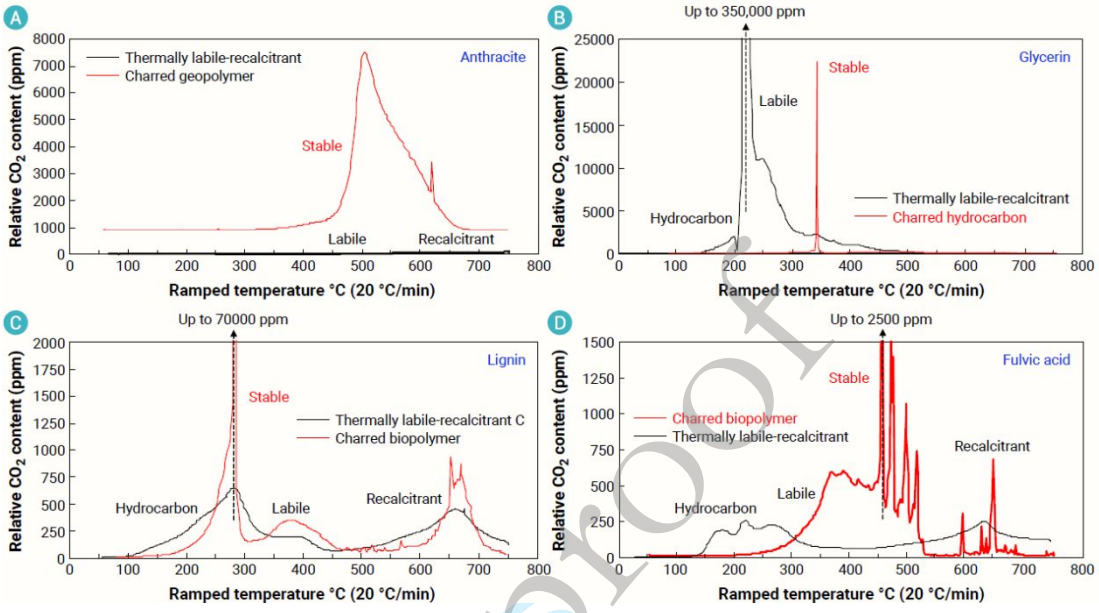

Figure 3. The CO_2 thermogram of selected OC reference materials on ramped temperatures of pyrolysis-combustion method. Pyrolysis generates thermally labile from hydrocarbon decomposition and biopolymer cracking and thermally recalcitrant from geopolymer cracking fractions. Combustion of pyrolysis residue generates thermally stable fractions. **A.** anthracite; **B.** glycerin; **C**. lignin; **D**. fulvic acid.

^{14}C age patterns to show selective preservation dynamics

The Yellow River course has undergone six large-scale changes, with the most recent occurring since AD 1850[46–47]. AMS ^{14}C dating of current Yellow River deltaic sediments at depths of 0–20 m (Fig. 1A) provides quantitative data to assess whether ancient or modern carbon is being sequestered in the coastal region in response to global changes (Fig. 4A).

Notably, the thermally labile-recalcitrant and stable OC fractions are 4,000–14,000 years older than the AD 1850 reference, while the labile-recalcitrant OC fractions are approximately 10,000 years younger than the thermally stable fractions (Table S2). Similarly, in the last glacial loess-paleosol sequence in western Chinese

Loess Plateau (Fig. 1B) thermally labile-recalcitrant fractions are approximately 20,000 years younger than thermally stable OC fractions (Fig. 4B, Table S2). These patterns show that OC in fluvial and eolian systems is selectively preserved by minerals as a result of intensive erosion, degradation, oxidation, and microbial respiration.

^{14}C age patterns to show mineral protection without microbial respiration

Rock varnish on limestone bedrock surface over karst landscape in subtropical SW China is an OC-rich veneer, comprising approximately 13-26% and 29-49% OC in two of our study areas, formed by fixation of OC compounds by Fe-Mn minerals (Fig. 1C). As erosion removes soil mass, bedrock becomes exposed, and varnish layers developed on newly exposed bedrock surfaces. In this context, the thermally labile-recalcitrant fractions of rock varnish OC yield AMS ^{14}C dates that are older than those of the thermally stable fractions (Fig. 4C, Table S3). Similarly, our previously obtained thermally labile-recalcitrant and thermally stable OC fractions from flood-induced sediments in caves within the warm-humid karst region of the central United States yielded identical ^{14}C dates[34] with similar trends (Fig. 4D, Table S3). In both cases, the results deviate from those expected on the basis of the Arrhenius equation. These reversed or identical age patterns imply OC cycling dynamics in which OC compounds are protected from microbial respiration, weathering, and oxidation by natural shielding mechanisms (Figs. 4C-4D).

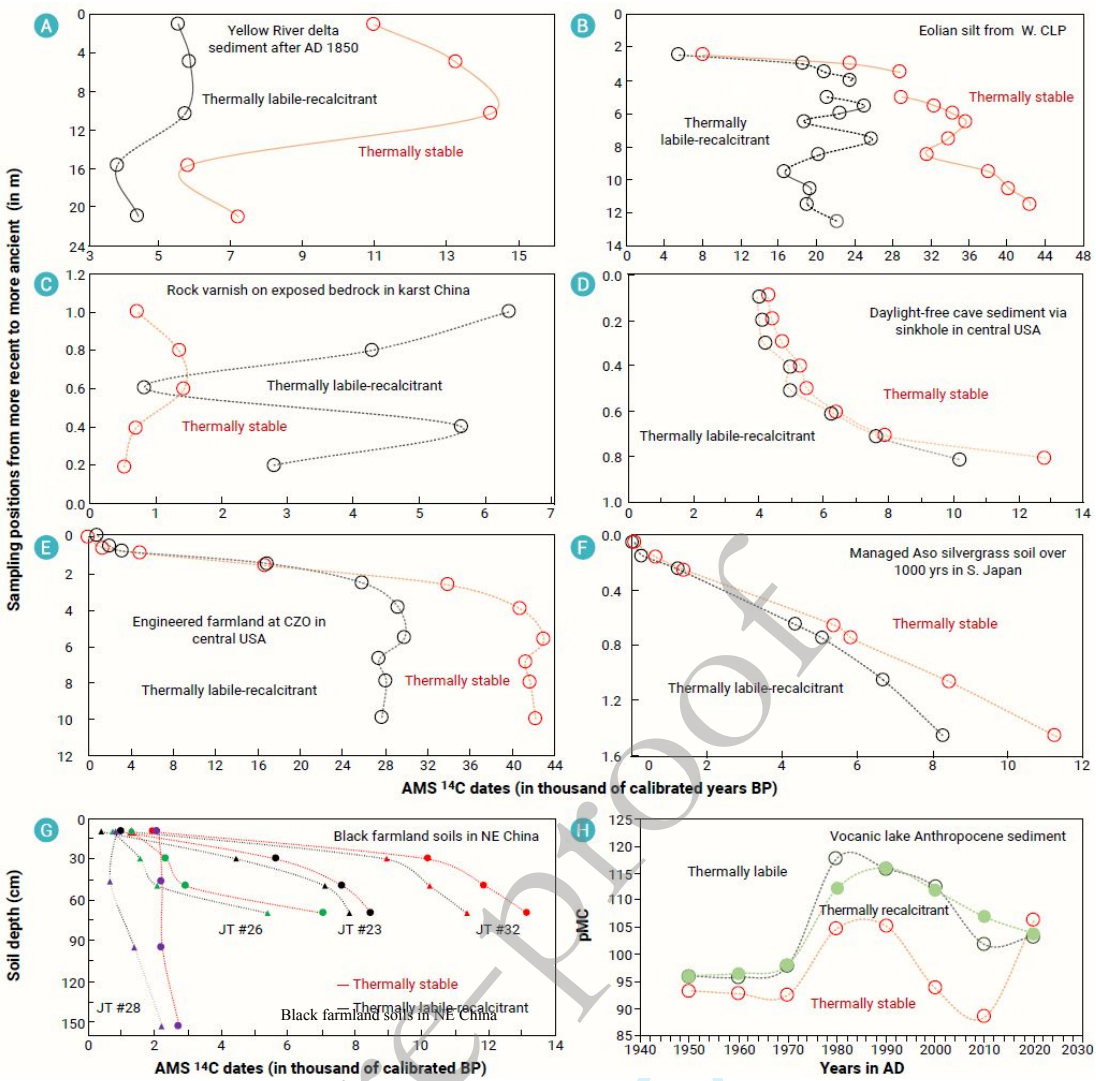

Figure 4. AMS ^{14}C age patterns of OC fraction cycling dynamics. **A-B**. Consistent with the first-order rate assumption of the Arrhenius equation, thermally stable and labile-recalcitrant OC fractions yield constant older-younger AMS ^{14}C age patterns indicating selective preservation dynamics. **D-D**. Contradicting the first-order reaction rate, as expressed by an Arrhenius relationship, thermally stable and labile-recalcitrant OC fractions yield reversed younger-to-older or identical AMS ^{14}C age patterns indicating protective dynamics; For sampling rock varnish: exposed bedrock base is set as 0 (m). **E-F**. Identically modern-aged AMS ^{14}C dates of thermally stable and labile-recalcitrant OC fractions in upper profiles and older-younger age offset patterns in lower profiles, revealing transition from unprotected to stabilized OC pools. **G**. AMS ^{14}C dates of thermally labile-recalcitrant and stable fractions exhibit closely-spaced younger-to-older age offsets up to 10000 years in JT #32 due to erosion and remains unchanged in JT #28 indicating OC accumulation. **F**. pMC of thermally labile, recalcitrant, and stable OC fractions captures atmospheric ^{14}C/^{12}C changes since AD 1950 with constant younger-to-older age offset. Reversely. in AD 2010 and 2020, thermally labile fraction is ~5% lower and stable fraction is ~2.5% higher than other fractions.

^{14}C age patterns to show unprotected to organo-mineral transition

Modern and identical AMS ^{14}C dates for thermally stable and labile-recalcitrant organic carbon fractions near the surface, along with consistent younger-to-older age

patterns in lower critical zone profiles at the central United States[36] and silvergrass farmland in southern Japan[48], reveal distinct pools of unprotected and mineral-protected OC (Figs. 4E-4F, Table S4). Ecosystems with high biological productivity produce abundant unprotected SOC in near-surface horizons, where no measurable microbial respiration-induced age offset is observed between thermally sensitive OC fractions. As unprotected OC is progressively fixed by minerals at greater soil depths, age offsets between thermally sensitive fractions emerge, consistent with recycling of carbon. These ^{14}C age pattern shifts provide valuable insights into how unprotected organic carbon progressively migrates into organo-mineral associations across different ecosystems.

^{14}C age patterns to show OC dynamics in heavily cultivated soils

Black mollisol farmland in cool-humid NE China is heavily cultivated (Fig. 2A). AMS ^{14}C dates of thermally labile-recalcitrant and stable OC fractions of four mollisol profiles in the Jiutai (JT) City District, Jilin Province, show closely spaced non-modern younger-to-older age patterns (Fig. 4G, Table S5). Among four farmlands, AMS ^{14}C age patterns of JT #32 and #23 profiles reveal severe OC erosion, indicated by large age increases over intervals of only 10 cm, while profile JT #28 shows remarkable OC accumulation, evidenced by consistent ages throughout the most soil profile (Fig. 4G).

^{14}C age patterns to show OC dynamics in high-closure lacustrine

A high-closure volcanic lake sediment (Fig. 2B), located adjacent to the black farmland profiles in the cool-humid climatic zone, captures Anthropocene sedimentation history spanning AD 1950–2020 by varve counting and measurements of ^{137}Cs, $^{240/239}Pu$, and ^{129}I anthropogenic radioisotope between 0 and 9 cm depths[49–51]. The depth of 0-1 cm depth is modeled as AD 2020, while depth of 8.3 cm was modeled as AD 1950[49–51]. The pMC values of thermally labile, recalcitrant, and stable OC

fractions reflect atmospheric $^{14}C/^{12}C$ changes since the beginning of the Anthropocene Epoch, with the exception of AD 2010 ± 3 years and AD 2020 ± 3 years. Specifically, in AD 2010, the pMC value of the thermally labile fraction is reversed approximately 5% lower (older) than that of the thermally recalcitrant fraction. In AD 2020, the pMC value of the thermally stable fraction is reversed approximately 2.5% higher (younger) than either the thermally labile or recalcitrant fractions (Fig. 4H, Table S6). These results demonstrate that high-resolution AMS ^{14}C dates and tracers of OC compounds in this drainage-free lake within the cool-humid forest ecosystem reveal how selective preservation mechanisms mainly stabilize different OC fractions over time.

DISCUSSION

To increase the ability of terrestrial ecosystems to store carbon and to sequester atmospheric CO_2 for climate change mitigation, both the long-term stability and high input of biosphere OC are equally important. To date, however, no numerical models have succeeded in predicting total SOC stability and turnover times[7–8], and current geochemical methods remain marginal—or are even incapable of verifying—different OC preservation mechanisms[5]. Our technology, which partitions thermally labile-recalcitrant and stable OC fractions for AMS ^{14}C dating while providing biochemical characterization and source origin information, offers benchmarks for verifying proposed selective and protective OC preservation mechanisms. We find that consistent with the first-order rate assumption of the Arrhenius equation, thermally labile-recalcitrant and stable OC fractions yield constantly younger-to-older AMS ^{14}C age patterns, verifying a selective preservation mechanism by minerals. This age pattern captures configuration of OC fractions following long and intense microbial respiration. In one case, AMS ^{14}C age offsets spanning 10^4-year ranges in the Yellow River deltaic fluvial and western Chinese loessland eolian silt profiles reveal that intensively respired

OC from erosion areas, transported via eolian and fluvial processes, is selectively preserved to form stabilized OC-mineral associations in the deposition areas. In the other case, age offsets spanning $10^{2\text{-}3}$-year ranges in farmland and high-closure lacustrine sediments indicate in-situ selective preservation mechanisms driven by local microbial respiration.

A striking observation is that thermally stable and labile-recalcitrant OC fractions yield random age patterns, including reversed younger-to-older and/or identical AMS ^{14}C ages. These patterns reflect the configuration of terrestrial OC compounds with variable or identical origins and without strong signals of microbial respiration. Such age patterns provide potential benchmarks for verifying OC protective mechanisms in terrestrial organo-mineral associations. In addition, in high-OC-stock ecosystems, both thermally labile-recalcitrant and stable fractions yield modern age signals in the rhizosphere and exhibit progressively larger younger-to-older age offsets toward deeper zones. These age patterns capture the configuration of terrestrial OC fractions transitioning from unprotected biopolymers to persistent organo-mineral associations, demonstrating this important transformative process.

Before asserting that pyrolysis-combustion for AMS ^{14}C dating technology offers the potential to verify OC cycling mechanisms currently only hypothesized in modeling studies, we conducted three experiments to reconcile uncertainties and concerns associated with this approach. The first experiment mixed two end-member reference materials composed predominantly of labile-recalcitrant or stable OC compounds with different ages to test whether their AMS ^{14}C dates are regulated by the dominant OC fractions. We mixed an older international reference materials of humic acid crystals with overwhelmingly dominant thermally stable fractions and international modern oxalic acid reference material with overwhelmingly dominant

thermally labile compounds. We also mixed an older animal protein residue with dominant thermally labile-recalcitrant compounds and younger international reference material of charcoal with dominant thermally stable compounds. AMS ^{14}C dating results confirm that the pyrolysis-combustion technology partitions labile-recalcitrant and stable OC fractions reasonably well, without significant transformation of labile-recalcitrant into stable OC fractions, at least in these two end-member tests (Table 1, Fig. 5).

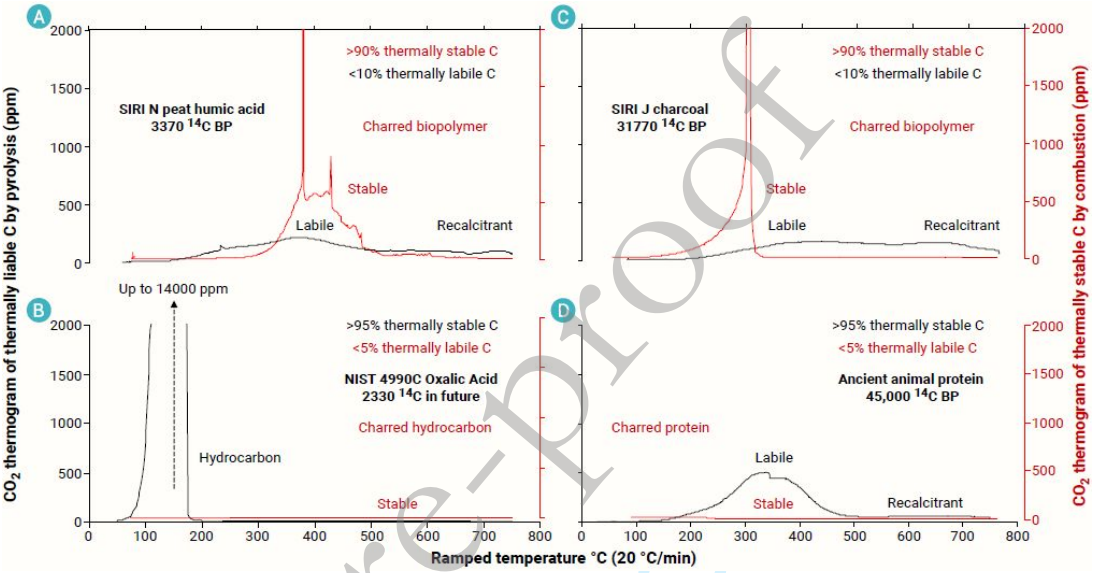

Figure 5. Thermographs of CO_2 of OC materials with different ages for two end-member mixture test. **A**. The 3370-year-old SIRI N peat humic acid yields overwhelmed stable (red) with small amount labile-recalcitrant (black) fractions. **B**. Modern oxalic acid standard of NIST 4990C yields overwhelmed labile fractions with trace amount recalcitrant and stable OC compounds. **A** and **B** are mixed for AMS ^{14}C dating test by using pyrolysis-combustion technology. **C**. The 31770-year-old SIRI J charcoal yields large amount stable and small amount labile-recalcitrant compounds. **D**. The 45000-year-old animal protein from a paleolithic site yields dominant amount labile and small amount recalcitrant and stable organics. **C** and **D** are mixed for test.

Table 1. AMS ^{14}C dates of two end member mixture test

Sample#	Wt (mg)	^{14}C age BP	± 1σ	IntCal20 BP	± 2σ
SIRI N humic acid	4.19	3370	25	3605	100
NIST OX II acid	3.83	-2330	20	-	
SIRI J charcoal	2.40	31770	1065	36285	2420
Old animal protein	15.9	45000	1800	47570	3875
Thermally labile-recalcitrant of SIRI N + OX II		-130	40	-	
Thermally stable of SIRI N + OX II		3360	40	3590	105
Thermally labile-recalcitrant of SIRI J + animal protein		41100	350	44085	670
Thermally stable of SIRI J + animal protein		38430	260	42415	220

The second experiment involved analyzing CO_2 thermograms from pyrolysis and combustion over a ramped temperature range of 40–750 °C, recorded by our IRGA device. We observed that the widely used Rock-Eval analysis for characterizing thermally sensitive OC fractions[38–41] shares fundamental principles with our pyrolysis-combustion technology for AMS ^{14}C dating[34].

We directly correlate our thermally labile fractions (<450 °C) and thermally recalcitrant OC fractions (>450 °C) to Rock-Eval's hydrocarbon-biopolymer and biopolymer fractions, respectively, and our thermally stable OC fractions to Rock-Eval's biopolymer-geopolymer fractions[42–45]. Specifically, two CO_2 thermograms were obtained from rock varnish OC samples: one sample exhibited the normal age pattern, with labile-recalcitrant OC fractions younger and stable OC fractions older over timescales of 10^2 years, while the other showed a reversed pattern, with labile-recalcitrant OC fractions older and stable OC fractions younger over timescales of 10^3 years (Fig. 4C). The CO_2 thermograms of rock varnish veneer OC samples exhibiting the normal age pattern reveal that thermally stable compounds contain a significant amount of charred labile-recalcitrant compounds, suggesting in-situ respiration on limited OC sources (Fig. 6A). In contrast, the CO_2 thermograms of samples showing reversed age patterns indicate that thermally stable compounds are not charred products of labile-recalcitrant fractions (Fig. 6B). In this case,

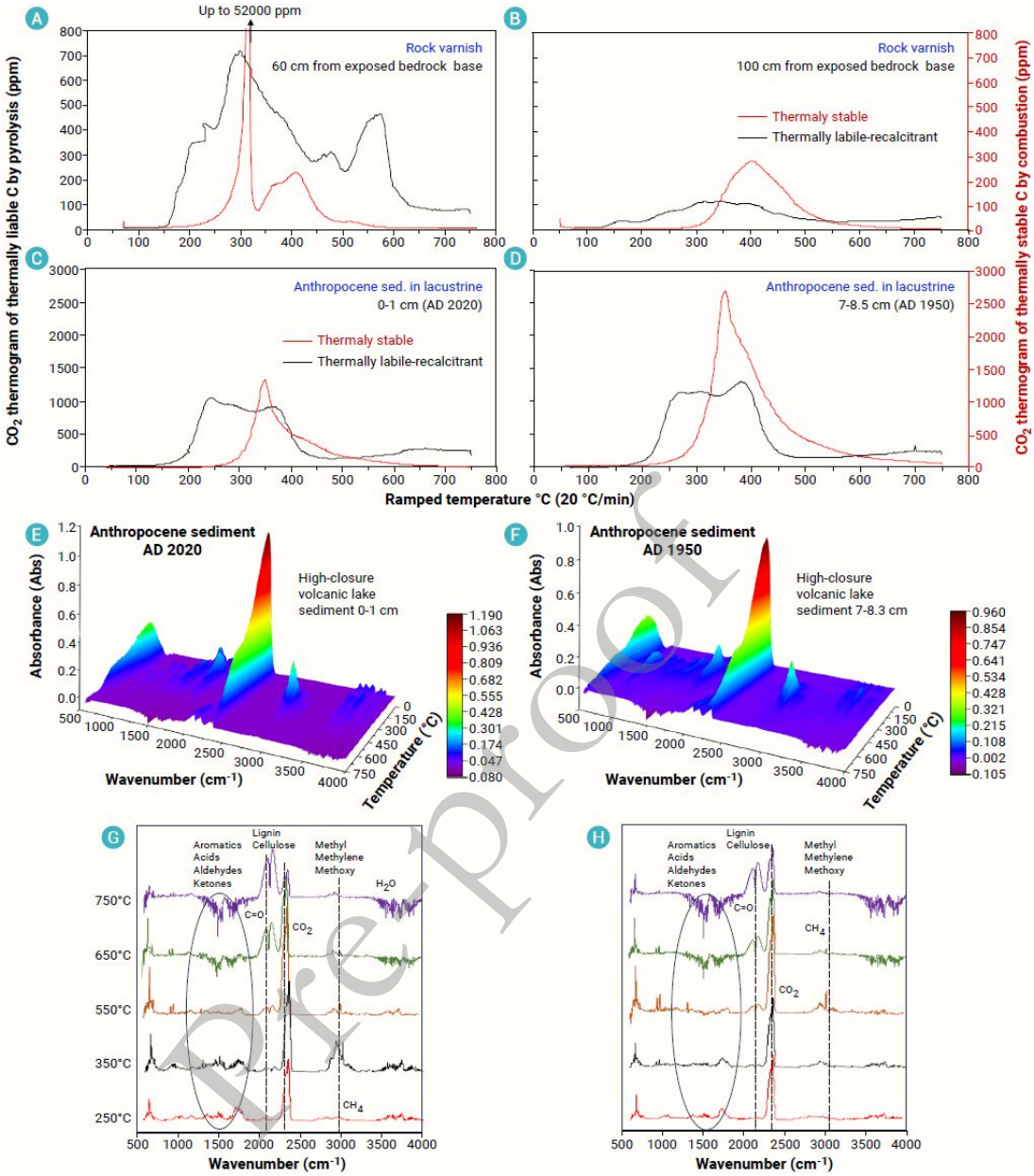

Figure 6. Origin and evolution of thermally labile-recalcitrant and stable OC compounds by interface of pyrolysis-combustion and online IRGA and FTIR methods.

labile-recalcitrant OC compounds may originate from old hydrocarbons sourced from deep sediments through karst cracks and sinkholes, while stable OC compounds may be derived from younger elemental carbon released by local wood burning. Both older and younger OC compounds are rapidly fixed by Fe-Mn oxides on the bedrock surface without significant microbial respiration.

Because the CO_2 thermograms of the Anthropocene samples from 0–1 cm (AD 2020) and from 7–8.3 cm (AD 1950) depths in the high-closure lake could not

differentiate the origins of labile and stable OC (Figs. 6C-6D), we conducted a third experiment. In this case, we analyzed gas-phase FTIR spectra to identify OC functional groups[52-54] that contribute to the higher pMC value (younger) in thermally stable than in labile and recalcitrant OC fractions. Comparation of selected FTIR spectra of 0-1 (AD 2020) and 7-8.3 cm (AD 1950) sedimentary samples show that pyrolysis products vary largely in similar absorbance bands with variable intensities in different temperature ranges (Figs. 6E-6F). Absorbance bands in 1900-1450 cm^{-1}, mainly for the stretching vibrations of aromatics, acids, aldehydes and ketones[52-53], are observed with the greater intensities in 0-1 cm sediment especially in 250-550 °C ranges, suggesting increasing aromaticity in AD 2020 sample (Figs. 6E-6F). Absorbance bands in 2000–2250 cm^{-1} indicate presence of CO, resulted from pyrolysis degradation of lignocellulosic structures[52-53], and intensity is lower in 250-550 and higher in 650-750 °C (Figs. 6G-6H). Finally, the absorbance bands at the region in 2850–3030 cm^{-1} reveal hydrocarbon gas consisting mainly of CH_4 due to small amount of methyl, methylene, and methoxy group decomposition (Figs. 6G-6H)[52,54]. Results of increasing aromaticity and high-temperature lignocellulose products in AD 2020 sample reveal that perhaps burning of forest wood with 30-50 years' life span produces aerosols causing higher pMC values in the thermally stable OC compounds (Fig. 4H).

CONCLUSION

We conclude that this novel technology, combined with Rock-Eval and FTIR spectra analyses, provides high precision results for verifying terrestrial OC preservation mechanisms that are currently known only from modeling simulations. In fluvial, eolian, and farmland ecosystems, thermally labile-recalcitrant and stable OC fractions exhibit constantly younger-to-older AMS ^{14}C age patterns across the 10^2–10^4-year range, exemplifying the selective preservation of OC compounds by minerals

under microbial respiration. In contrast, the same OC fractions from rock varnish and flood sediments in karst cracks and sinkholes display reversely older-to-younger or identical ^{14}C age patterns, illustrating the protection of OC compounds by minerals in the absence of intensive respiration. In high OC-stock ecosystems, these fractions yield uniformly modern ages in rhizosphere but show younger-to-older age patterns in deeper zones, reflecting the dynamics of naturally unprotected bio-OC progressively transforms into OC-mineral associations. The CO_2 thermograms obtained via the IRGA and OC functional groups by FTIR analysis provide biochemical evidence to assess origin of terrestrial OC compounds, thereby improving our understanding of their age patterns.

These results also show that OC decay dynamics by using this technology follows the first-order kinetics in the activation energy distribution that is independent from experimental conditions. Because the Arrhenius equation ($k = Ae^{-Ea/RT}$) that considers the pre-exponential factor or the Arrhenius factor (A) and the molar activation energy (Ea) to be temperature independent constants[55] applies to our works, this updated technology could provide reliable Ea values for variable OC thermal fractions. The molar activation energy (Ea) is a proxy for carbon bond strength of OC components, which regulate their stability in the terrestrial ecosystems[5, 21]. In future studies, AMS ^{14}C age patterns among thermally sensitive OC fractions can be further compared with the Ea values not only to identify types but also to quantify terrestrial OC cycling dynamics.

REFERENCES

1. Friedlingstein, P. et al., Global carbon budget 2023. Earth Syst. Sci. Data 15, 5301-5369 (2023).
2. Davidson, E.A., Janssens, I.A. Temperature sensitivity of soil carbon decomposition and feedbacks to climate change. Nature 440, 165-173 (2006).
3. Crowther, T.W. et al. Quantifying global soil carbon losses in response to warming. Nature 540, 104-108 (2016).

4. Wang, M.M. et al., Global soil profiles indicate depth-dependent soil carbon losses under a warming climate. Nat. Commun. 13, 5514 (2022).
5. Hemingway, J.D., Rothman, D.H., Grant, K.E., Rosengard, S.Z., Eglinton, T.I., Derry, L.A. & Galy, V.V. Mineral protection regulates long-term global preservation of natural organic carbon. Nature 570, 228-231 (2019).
6. Schmidt, M.W.I., Torn, M.S., Abiven, S., Dittmar, T., Guggenberger, G., Janssens, I.A., Kleber, M., Ko¨gel-Knabner I., Lehmann, J., Manning, D.A.C., Nannipieri, P., Rasse, D.P., Weiner, S., Trumbore, S.E. Persistence of soil organic matter as an ecosystem property. Nature 478, 49-56 (2011).
7. Kleber, M.K. et al., Dynamics interactions at the mineral-organic matter interface. Nature Reviews Earth & Environment 2, 403-421 (2021).
8. Moore, O.W., Curti, L., Woulds, C., Bradley, J.A., Babakhani, P., Mills, B.J.W., Homoky, W.B., Xiao, K.Q., Bray, A.W., Fisher, B.J., Kazemian, M., Kaulich, B., Dale, A.W., Peacock, C.L. Long-term organic carbon preservation enhanced by iron and manganese. Nature 621, 312-317 (2023).
9. Leinweber, P. & Schulten, H.R. Advances in analytical pyrolysis of soil organic matter. J. Anal. Appl. Pyrolysis 49, 359–383 (1999).
10. Plante, A.F., Fernández, J.M. & Leifeld, J. Application of thermal analysis techniques in soil science. Geoderma 153, 1–10 (2009).
11. Kleber, M. What is recalcitrant soil organic matter? Environ. Chem. 7, 320-332 (2010).
12. Davidson, E.A., and Janssens, I.A. Temperature sensitivity of soil carbon decomposition and feedbacks to climate change. Nature, 440, 165 (2006). doi:10.1038/NATURE04514
13. Bosatta, E., Agren, G.I. Soil organic matter quality interpreted thermodynamically. Soil Biol. Biochem., 31, 1889 (1999). doi:10.1016/S0038- 0717(99)00105-4.
14. Fierer, N., Craine, J.M., McLauchlan, K., Schimel, J.P. Litter quality and the temperature sensitivity of decomposition. Ecology, 86, 320 (2005). doi:10.1890/04-1254.
15. Conant, R.T., Drijber, R.A., Haddix, M.L., Parton, W.J., Paul, E.A., Plante, A.F., Six, J., Steinweg, J. M. Sensitivity of organic matter decomposition to warming varies with its quality. Glob. Change Biol., 14, 868 (2008). doi:10.1111/J.1365-2486.2008.01541.X.
16. Feng, X.J. and Simpson, M.J. Temperature responses of individual soil organic matter components. J. Geophys. Res., 113, G03036 (2008). doi:10.1029/2008JG000743.
17. Zhang, Y.S., Galy, V., Yu, M., Zhang, H.L., Zhao, M.X., Terrestrial organic carbon age and creativity in the Yellow River fueling efficient preservation in marine sediments. Earth and Planetary Science Letters 585 (2022) 117515 (2022).
18. Brady, N.C. and Weil, R.R. The Nature and Properties of Soils (Prentice Hall: Upper Saddle River, NJ (2008).
19. Schulten, H-R. and Schnitzer, M. Chemical model structures for soil organic matter and soils. Soil Sci. 162, 115 (1997). doi:10.1097/ 00010694-199702000-00005.
20. Swift, R. Macromolecular properties of soil humic substances: fact, fiction and opinion. Soil Sci., 164, 790 (1999). doi:10.1097/00010694- 199911000-00003.
21. Hemingway, J.D., Rothman, D.H., Rosengard, S.Z. & Galy, V.V. Technical note: an inverse method to relate organic carbon reactivity to isotope composition from serial oxidation. Biogeosciences 14, 5099–5114 (2017).
22. Gutfreund, H. Kinetics for the Life Sciences (Cambridge University Press: Cambridge, UK) (1995).
23. Fierer, N., Colman, B.P., Schimel, J.P., Jackson, R.B. Predicting the temperature dependence of microbial respiration in soil: a continental-scale analysis. Global Biogeochem. Cy., 20, GB3026 (2006). doi:10.1029/2005GB002644.
24. Keiluweit, M., Nico, P.S., Johnson, M.G., & Kleber, M. Dynamic molecular structure of plant biomass-derived black carbon (biochar). Environ. Sci. Technol. 44, 1247-1253 (2010).

25. Williams, E.K., Rosenheim, B.E., NcNichol, A.P., Masiello, CA. Charring and non-additive chemical reactions during ramped pyrolysis: Applications to the characterization of sedimentary and soil organic material. Organic Geochemistry 77, 106-114 (2014).
26. Rosenheim, B.E., Day, M.B., Domack, E, Schrum, H., Benthien, A., Hayes, J.M. Antarctic sediment chronology by programmed-temperature pyryolysis: Methodology and data treatment. Geochemistry, Geophysics, Geosystems 9. Q04005, doi:10.1029/2007GC001816 (2008).
27. Ginnane C.E., Turnbull, J.C., Naeher, S., Rosenheim, B.E., Venturelli, R.A., Phillips, A.M., Reeve, S., Parry-Thompson, J., Zondervan, A., Levy, R.H., Yoo, K.-C., Dunbar, G. Calkin, T., Escutia, C., Pastor, J.G. Advancing Antarctic sediment chronology through combined ramped pyrolysis oxidation and pyrolysis-GC-MS. Radiocarbon, 00. DOI:10.1017/RDC.2023.116 (2024).
28. Zigah, P.K., Minor, E.C., McNIchol, A.P., Xu, Li, Werne, J.P. Constraining the sources and cycling of dissoved organic carbon in a large oligotrophic lake using radiocarbon analyses. GCA 208, 102-118 (2017).
29. Hedges, J. The formation and clay mineral reactions of melanoidins. Geochim. Cosmochim. Acta 42, 69–76 (1978).
30. Piccolo, A. The supramolecular structure of humic substances. Soil Sci., 166, 810 (2001). doi:10.1097/00010694-200111000-00007.
31. Sutton, R. and Sposito, G. Molecular structure in soil humic substances: the new view. Environ. Sci. Technol., 39, 9009 (2005). doi:10.1021/ ES050778Q.
32. Marschner, B. et al. How relevant is recalcitrance for the stabilization of organic matter in soils? J. Plant Nutr. Soil Sci. 171, 91–110 (2008).
33. Kleber, M. & Johnson, M. G. Advances in understanding the molecular structure of soil organic matter: implications for interactions in the environment. Adv. Agron. 106, 77–142 (2010).
34. Wang, H., Hackley, K.C., Panno, S.V., Coleman, D.D., Liu, J. C-L., Brown, J. Pyrolysis combustion 14C dating of soil organic matter. Quaternary Research 60, 348-355 (2003).
35. Wang, H., Ambrose, S., Headman, K., and Emerson, T. AMS 14C dating of human bones using sequential pyrolysis and combustion of collagen. Radiocarbon 52 (1) 157-163 (2010).
36. Wang, H., Stumpf, A.J., Kumar, P., Labile and inert carbon cycling dynamics in the Critical Zone Observatory in Illinois, USA. Radiocarbon 60, 989-999 (2018). DOI:10.1017/RDC.2018.31.
37. Cheng, P., Zhou, W.J., Wang, H., Lu, X.F., Du, H. 14C dating of soil organic carbon (SOC) in loess-paleosol using sequential pyrolysis and accelerator mass spectrometry (AMS). Radiocarbon 55, 563-570 (2013).
38. Disnar, J.R., Guillet, B., Keravis, D., Di-Giovanni, C., Sebag, D. Soil organic matter (SOM) characterization by Rock-Eval pyrolysis: scope and limitations. Organic Geochemistry 34, 327-343 (2003).
39. Baudin, F., Disnar, J-R., Aboussou, A., Savignac, F. Guidelines for Rock-Eval analysis of recent marine sediments. Organic Geochemistry 86, 71-80 (2015).
40. Sebag, D., Verrecchia, E.P., Cecillon, L., Adatte, T., Albrecht, R., Aubert, M., Bureau, F., Cailleau, G., Copard, Y., Decaens, T. Disnar, J.-R., Hetenyi, M., Nyilas, T., Trombino, L., Dynammics of soil organic matter based on new Rock-Eval indices. Geoderma 284, 185-203 (2016).
41. Lamoureux-Var, V., Bouton, N., Espitalie, J., Benoit, Y. 2023. Chapter 2. Principles and methods. In The Rock-Eval Method ed. by Baudin, F. pp. 11-27. ISTE London, UK and Wiley Hoboken NJ USA (2023).
42. Albrecht, R., Sebag, D., Verrecchia, E. Organic matter decomposition: bridging the gap between Rock–Eval pyrolysis and chemical characterization (CPMAS 13C NMR). Biogeochemistry 122, 101–111. https://doi.org/10.1007/s10533-014-0033-8 (2015).

43. Barré, P., Plante, A.F., Cécillon, L., Lutfalla, S., Baudin, F., et al. The energetic and chemical signatures of persistent soil organic matter. Biogeochemistry 130, 1–12. https://doi.org/10.1007/s10533-016-0246-0 (2016).
44. Carrie J., Sanei H., Stern G. Standardization of Rock–Eval pyrolysis for the analysis of recent sediments and soils, Organic Geochemistry 46 (2012) 38–53, doi:10.1016/j.orggeochem.2012.01.011 (2012).
45. Cécillon L., Baudin F., Chenu C., Houot S., Jolivet R., et al. A model based on Rock-Eval thermal analysis to quantify the size of the centennially persistent organic carbon pool in temperate soils, Soil Biology and Biochemistry, Volume 117, February 2018, Pages 117-124 (2018).
46. Pang, J.Z. and Si, S.H. The estuary changes of Huanghe River I. Changes in modern time. Oceanologia et Liminologia Sinica 10, 136-141 (1979).
47. Pang, J.Z. and Jiang, M.X. On the evolution of the Yellow River estuary (Part II). Transactions of Oceanology and Limnology 4, 1-13 (2003).
48. Howlett, D.S., Toma, Y., Wang, H., Sugiyama, S., Yamada, T. Nishiwaki, A., Fernandez, F., Stewart, J.R. Soil carbon source and accumulation over 12,000 years in a semi-natural Miscanthus sinensis grassland in southern Japan. Caten, 104, 127–135 (2013).
49 Chu, G., Gu, Z. & Xu, B. Varve chronology and radiometric dating (137Cs, 210Pb) from the Sihailongwan Maar, Northeastern China (In Chinese with English Abstract). Quaternary Sciences 25, 202–207 (2005).
50. Mingram, J., Stebich, M., Schettler, G., Hu, Y., Rioual, P., Nowaczyk, N., Dulski, P., You, H., Opitz, S., Liu, Q., Liu, J., 2018. Millennial-scale East Asian monsoon variability of the last glacial deduced from annually laminated sediments from Lake Sihailongwan, N.E. China. Quat. Sci. Rev. 201, 57–76.
51. Han, Y.M, An, Z.S, Lei, D.W. & Zhou, W.J. The Sihailongwan Maar Lake, northeastern China as a candidate Global Boundary Stratotype Section and Point for the Anthropocene Series. The Anthropocene Review 1-24 (2023). ttps://doi.org/10.1177/20530196231167019
52. Özsin and Pütün, Kinetics and evolved gas analysis for pyrolysis of food processing wastes using TGA/MS/FT-IR. Waste Manag. 64, 315 (2017).
53. Li, T.T., Song, F.H., Zhang, J., Liu S.S., Xing, B.S., Bai, Y.C. Pyrolysis characteristics of soil humic substance using TG-FTIR-MS combined with kinetic models. Science of the total environment 698 (2020) 134237.
54. Ma, Z., Chen, D., Jie, G., Bao, B., Zhang, Q. Determination of pyrolysis characteristics and kinetics of palm kernel shell using TGA–FTIR and model-free integral methods. Energy Convers. Manag. 89, 251–259 (2015).
55. Arrhenius, S. A. On the heat of dissociation and the influence of temperature on the degree of dissociation of the electrolytes. Z. Phys. Chem. 4, 96–116 (1889). doi:10.1515/zpch-1889-0408. S2CID 202553486.

FUNDING AND ACKNOWLEDGMENTS

This research was supported by NSFC Grant No. 41991253 and 42072206, LSKJ202203301, and NSFC No. U2243208. Authors thank Mr. Bing Li, Zhen Zhang, Dr. Jianghu Lan, and Dr. Deming Lei for field works. We also thank two anonymous reviewers' valuable suggestions and comments.

AUTHOR CONTRIBUTIONS

Conceptualization: H WANG, P CHENG, Y YANG, XF LU, YM HAN, XL HOU, L LIU, WJ ZHOU, ZS AN
Methodology: H WANG, YN LIU, GD MING, XF LU, H DU, F XIAN, SY ZHU, YM SUN, TH Liu, XL ZHAO, F XIAN, L LIU, XL HOU
Investigation: H WANG, XF Gao, Y YANG, YN LIU, J CAO, DX LI, KL ZHANG, BS CUI.
Visualization: Y YANG, PX SHU, GD MING, H DU, PX SHU
Supervision: H WANG, XF LU, KL ZHANG, BS CUI
Writing—original draft: H WANG, P CHENG, WJ ZHOU, ZS AN
Writing—review & editing: XL HOU, XL ZHAO, WJ ZHOU, ZS AN

DECLARATION OF INTERESTS

The authors declare that they have no known competing financial interests or personal relationships that could have appeared to influence the work reported in this paper.